TRIBHUVAN UNIVERSITY

INSTITUTE OF ENGINEERING

PULCHOWK CAMPUS

B-05-BME-2018/2023

STUDY AND DESIGN OF THERMAL MANAGEMENT SYSTEM OF LITHIUM-ION BATTERY MODULE.

BY:

ABHISHEK UPRETY (075BME005)

DAYA BANDHU GHIMIRE (075BME016)

SAROJ NEUPANE (075BME040)

A PROJECT REPORT

SUBMITTED TO THE DEPARTMENT OF MECHANICAL AND AEROSPACE ENGINEERING IN PARTIAL FULFILLMENT OF THE REQUIREMENT FOR THE DEGREE OF BACHELOR IN MECHANICAL ENGINEERING

DEPARTMENT OF MECHANICAL AND AEROSPACE ENGINEERING
LALITPUR, NEPAL

APRIL 2023

COPYRIGHT

TRIBHUVAN UNIVERSITY

INSTITUTE OF ENGINEERING,

PULCHOWK CAMPUS

DEPARTMENT OF MECHANICAL AND AEROSPACE ENGINEERING

The undersigned certify that they have read, and recommended to the Institute of Engineering for acceptance, a project report entitled "STUDY AND DESIGN OF THERMAL MANAGEMENT SYSTEM OF LITHIUM-ION BATTERY MODULE" submitted by Abhishek Uprety, Daya Bandhu Ghimire and Saroj Neupane in partial fulfillment of the requirements for the degree of Bachelor of Mechanical Engineering.

_____

Supervisor, Dr. Sanjeev Maharjan

Assistant Professor

Department of Mechanical and Aerospace Engineering

_____

External Examiner, Er. Dipesh Poudel

Training Manager

Sipradi Trading Pvt. Ltd.

_____

Committee Chairperson, Assoc. Prof. Dr. Surya Prasad Adhikari

Head of the Department of Mechanical and Aerospace Engineering

_____

Date

ABSTRACT

World is rapidly transforming into the age of Electric Vehicle technology. This is also associated with green and clean transportation technology. Lithium-ion batteries are rechargeable energy storage devices used in electrical vehicles due to high power density, low self-discharge, high efficiency, long life cycle etc. However, there is change in temperature during the charge/discharge cycle of operation due to heat generation. And, it is necessary to maintain the temperature of battery within specific range for the safety and life of the battery by adopting proper thermal management system. In this project, we aim to study and analyze thermal management systems for lithium-ion battery modules. For this purpose, we have conducted numerical study of unit cell module air cooling system using steady state Conjugate Heat Transfer in ANSYS Fluent 2022R1. Experimental setup is also developed for unit cell module air cooling. And, comparative study between experimental and numerical solution is conducted based on cell average temperature. Numerical analysis of 3S3P module air cooling system is conducted for four different flow channel configurations and varied velocities for obtaining efficient system. Numerical study of 3S3P module cold plate liquid cooling system is also conducted with four different flow channel configurations and varied flow velocities for obtaining suitable cold plate liquid cooling on basis of cell average temperature and temperature distribution in system. For a unit cell, it is found that the cell average temperature reaches stable value after certain flow velocity. There is a decrease in temperature due to an increase in velocity from 0.2 m/s to 4.3m/s for unit cell module air cooling system. From four different configurations of air cooling, SIDO configuration has less value of cell average temperature with varied velocity from response surface analysis and CHT simulation. Average cell temperature of cobweb type is least for the same coolant inlet velocity among four different liquid cold plate configurations. It is also found that temperature distribution using cobweb type cold plate is uniform at lower pressure.

ACKNOWLEDGEMENT

At first, we express our deepest gratitude towards the **Department of Mechanical and Aerospace Engineering,** IOE, Pulchowk Campus, Lalitpur, for providing us with the opportunity to work on a project to explore, enhance and apply knowledge, skills that we have gained throughout our Bachelor of Mechanical Engineering. We are thankful to the Head of Department**, Associate Professor Dr. Surya Prasad Adhikari**. Similarly, we would like to thank our supervisor, **Associate Professor Dr. Sanjeev Maharjan**, for his guidance and motivation. It certainly would not have been possible without him. We are very thankful to **Er. Denish Khatiwada** for his insightful remarks on this project. We would also like to thank **Robotics Club Pulchowk Campus** for their continuous support in creating a better workplace for the development of our experimental setup and conducting it. Our special gratitude goes to **the Center for Energy Studies** for providing the workspace for conducting numerical analysis and the measuring device required for our experiment.

Finally, we would also like to thank teachers, friends, seniors, and others who helped us.

Abhishek Uprety (075BME005)
Daya Bandhu Ghimire (075BME016)
Saroj Neupane (075BME040)

TABLE OF CONTENTS

LIST OF FIGURES

LIST OF TABLES

LIST OF ACRONYMS AND ABBREVIATIONS

EV	Electric Vehicles
HEV	Hybrid EV
LFP	Lithium Iron Phosphate
LCO	Lithium Cobalt Oxide
BTMS	Battery Thermal Management System
PCM	Phase Change Material
UBS	Union Bank of Switzerland
PVC	Poly-Vinyl Chloride
NiMH	Nickel-Metal Hydride
IP	Ingress Protection
NMC	Lithium Nickel Manganese cobalt oxide
IEC	International Protection Marking
P2D	Pseudo Two-Dimensional Model
SP	Single Particle Model
RC	Resistor-Capacitor
SOC	State of Charge
HPPC	High Pulse Power Characterization
ECM	Equivalent Circuit Model
NCA	Lithium nickel cobalt aluminum oxide
NASA	National Aeronautics and Space Administration
CALCE	Center for Advanced Life Cycle Engineering
LTO	Lithium Titanate
CFD	Computational Fluid Dynamics
MAT	Maximum Temperature
MATD	Maximum Temperature Difference
CAD	Computer Aided Design
SIDO	Single Input Double Output
SISO	Single Input Single Output
3S3P	3 Series 3 Parallel
SWs	SolidWorks

CHAPTER ONE: INTRODUCTION

1.1 Background

Lithium-ion has a high energy density, more cycle life, and fast-charging capabilities, but they also produce heat when used. If heat is not adequately dissipated, it can induce thermal runaway, impair battery performance and lifespan, and even lead to safety issues like fires and explosions. Battery manufacturers have created several cooling methods to regulate the heat developed by lithium-ion batteries to address this issue. A properly cooled battery can tolerate more charge and discharge cycles before deteriorating.

A well-designed lithium-ion battery cooling system can improve battery performance, boost safety, and extend battery longevity. The design of a lithium-ion battery cooling system is determined by the application and needs. For electric vehicles, the cooling system must be lightweight, compact, and efficient to have the least impact on the vehicle's range and performance. Air cooling is one method of regulating the heat created by lithium-ion batteries, which involves moving cool air over the battery cells to disperse heat. With fans or other air-moving devices, air is circulated through the battery pack. As air rushes over the battery cells, it absorbs heat and transports it away, allowing the battery to operate within a safe operating temperature range. Liquid cooling is employed when higher current performance is required. One of the most common cooling systems is liquid cooling, which employs a coolant to absorb and convey excess heat from the battery. The coolant travels through the battery pack's network of tubes or channels, exchanging heat with the battery cells and dispersing it to the outside environment.

Parametric studies are being done to fully understand the different parametric behavior on performance of a modules. Despite significant advancements in cooling technologies, particularly in recent years, there is still much more to analyze to fully compare them. Due to this reason, investigation in this project is done to have a better understanding of the comparative behavior of different cooling technologies.

1.2 Problem statement

Different methods have been practiced for maintaining the temperature of battery modules. Broader classification of BTMS has been done on different basis like power consumption, heat transfer medium, cell configurations (Tete et al., 2021) . The cooling systems are optimized for different parameters. Various kinds of optimizations are built specific to the system limited by battery type, design space, design parameters, heat flux etc. These optimal techniques cannot be compared to each other at all. Hence, there is a need for a standard module about which the cooling systems are to be compared.

This project aims to comparative study between numerical analysis and experimental results of unit cell module air cooling on cell average temperature. This project performs comparative analysis for four different configurations of cold plate liquid cooling on the basis of cell average temperature and pressure drop with response coolant flow velocity for 3S33P module. It also aims for comparative analysis for four different configurations of air-cooling channel with varying velocity based on cell average temperature with response inlet flow velocity for 3S3P module.

1.3 Objectives

1.3.1 Main objective

To study and design the thermal management system of lithium-ion battery modules.

1.3.2 Specific objectives

1. To implement heat generation model of Lithium-ion cell.
2. To develop unit cell module air cooling system, perform numerical analysis and compare with experimental results on the basis of cell average temperature.
3. To develop cold plate for module cooling for 3S3P module of four different configurations, perform parametric analysis and make comparative study between them on basis of cell average temperature and pressure drop.
4. To develop air cooling system of a 3S3P module of four different configurations, perform parametric analysis, and make comparative study between them on basis of cell average temperature.

1.4 Scope and Limitation of work

The scope of this project includes:

1. Design of air-cooling system for unit cell and 3S3P module and cold plate liquid cooling for 3S3P module.
2. Comparative study between numerical analysis and experimental results of unit cell module air cooling on cell average temperature.
3. Comparative study of four different cold plate liquid cooling system channel for 3S3P module on basis of cell average temperature, pressure dop with response to coolant inlet velocity
4. Comparative study of four configurations of air-cooling system channel for 3S3P module on basis of cell average temperature with response to inlet airflow velocity.

The limitation of this project includes:

1. System greater than 3S3P is not considered.
2. Our input parameters only include flow velocity with different flow channels and output response is only linked with cell average temperature.
3. Experimental analysis of 3S3P module has not been conducted.

CHAPTER TWO: LITERATURE REVIEW

2.1 Electric Vehicle and Battery

The world is now transforming into electric drives and electric vehicle technology. Electric vehicles are linked with green development and a decrease in harmful emissions (Manzetti & Mariasiu, 2015). EV batteries differ from batteries used in laptops and mobile phones in that they should control powerful batteries in a restricted size and weight (Garcia-Valle and Lopes 2013). Lithium batteries for hybrid and plug in hybrid electric vehicles, as well as power system storage and backup, are examples of applications (Gregory L. Plett, 2015).Because of their enormous power storage capacity and excellent energy density/weight ratio, lithium-ions are assuming lead as energy supply and storage devices in these vehicles (Manzetti & Mariasiu, 2015). The efficiency and safety of batteries are two important considerations. Electric vehicles make extensive use of battery cooling technology. Tesla, for example, employs liquid cooling & Nissan leaf air cooling technologies. Many mishaps involving catching fire of ola bikes have recently been reported.

Under the increasing pressure of emission levels legislation, energy scarcity, and high gasoline and diesel prices, electric vehicles (EVs) as well as hybrid electric vehicles (HEVs) with extremely effective drive systems and green power energy are feasible alternatives to standard vehicles powered by combustion engines. When the electric motor is turned on, EVs create no noise and no harmful emissions (Manzetti & Mariasiu, 2015).

According to Bloomberg, all cars will be replaced by EVs by 2040. With EVs, the motor serves as the primary mover, just as the engine in any diesel or petrol engine. In a combustion engine, the fuel storage tank stores energy, whereas in an electric vehicle, the battery stores energy. As a result, the battery is critical in EVs. Because of its high thermal density, powerful and long cycle, lithium ions are commonly utilized in EV batteries. They, however, are assumed to be susceptible to changes in parameters such as vibration, surrounding temperature, and pressure. The battery has an efficiency problem since heat causes it to lose efficiency owing to internal resistance (Lai et al., 2015).Hence. Lithium batteries for hybrid and electric vehicles, as well as power system storage and backup, are examples of applications.

2.2 Lithium-ion Battery

Lithium-ion is an active substance that ranks first in the electrochemical series. As a result, the potential of electrons lost by lithium is larger than that of other elements such as Mg, Al, and so on. They also offer a better power density, which allows for longer battery life in lighter packs. As a result, lithium ions are more commonly used as rechargeable batteries than other batteries, Lithium Nickel Manganese Cobalt Oxide (NMC), Lithium Iron Phosphate (LFP), Lithium Nickel Cobalt Aluminum Oxide (NCA), Lithium Cobalt Oxide (LCO), Lithium Manganese Oxide (LMO), and Lithium Titanate are some common lithium-ion batteries (LTO). The most common type of lithium-ion battery is LCO, which is widely used in mobile phones, laptop computers, cameras, and other electronic devices. Temperature, charge/discharge rate, ambient conditions, and vibration all have an impact on battery performance. Temperature distribution is one of the most important aspects. Several models can be used to determine the heat production or temperature built into the batteries. Other common models are the Newman model, which may replicate the temperature field in battery systems, and Bernardi's model, which provides the battery's energy equation.

2.3 Electrical model

Electrical models have a significant role in predicting battery dynamic characteristics. Various parameters such as SOC, voltage, current is calculated, and electric response is simulated and validated by this model. Electrical models result is helpful for proper battery management system along with assistance in thermal management of battery.

Battery electrochemical modeling provides a thorough knowledge of the physical and chemical processes that occur within the battery for constructing a cell (Panchal et al., 2018). It is a guide for design and manufacture of batteries. These models are based on electrochemical kinetics and transport equations that govern the internal electrochemical processes of the battery. The first model developed by Newman and Tiedemann was based on porous electrode theory. In his concept, the electrode is a mixture of the electrolytic mixture and the solid matrix. The matrix is represented by small spherical particles in which lithium ions distribute and respond on the sphere's face. According to (Jeon et al. 2014) the porous electrode theory, it is a multi-scale model made up of two non - dimensional geometries. A one-dimensional

geometry, at first, contains three sequentially connected straight objects, namely anode part, separator part, and cathode part. This resolves the electrical and ion potentials, as well as the solution concentration. In the second, two rectangles form a two-dimensional design to solve the Li-ion content inside the electrode components. A unit spherical object represents an individual electrode. Different parameters describing chemical composition need to be found to have real time implementation. The small particle layer and electrode are disjoined in the Newman P2D model. Lithium preservation is solved in particle layer domain. The spherical particle diffusion is governed by Fick's law.

In the electrode region, mass conservation and charge conservation are solved on the principles of transport mechanisms, thermodynamics, electrochemistry. Furthermore, electrochemical models frequently incorporate a large number of partial differential equations that necessitate a large amount of computation (K. Liu et al., 2019). In reduced electrochemical model the objective of model reduction is to approximate governing PDE (partial differential equations) in lower order ODE which can be easily solved by simulation software (Fan et al. 2018). However, because of the model's complexity, site accuracy is low when implemented in vehicle control systems. First, values of design parameters along with electrochemical kinetic variables must be acquired (Zhang et al., 2017).

Electrical circuit models are models comprising of mathematical and physical models. To overcome the computational time and on-site accuracy circuit model is used. They are simple, accurate and easy to implement (Barcellona et.al 2017). The widely used electric model are equivalent circuit model (ECM).

This model has not explained dynamic characteristics of battery. By considering the polarization properties of a battery to get accurate results, the use of an RC network with internal resistance is done. These are known as 'Thevenin' models (Fotouhi et al., 2016). The figure below is 1 RC ECM.

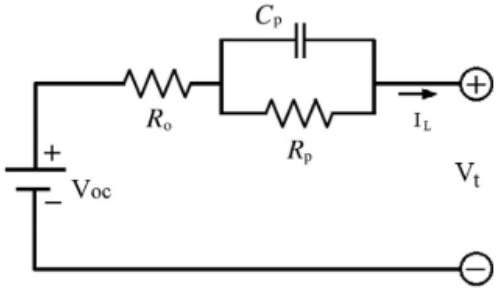

Figure 2-1: One RC-model (Fotouhi et al., 2016)

The ohmic resistance of the battery is represented by resistor Ro. C1 is the equivalent polarization capacitance, and R1 is the equivalent polarization resistance, which models the chemical diffusion of the electrolyte with the battery. Using the number of RC network to the battery model improves accuracy while increasing complexity. When computing effort and time are critical, a tradeoff is required (Fotouhi et al., 2016). Two RC pairs are usually enough to capture the system concentration and activation polarization of cells.

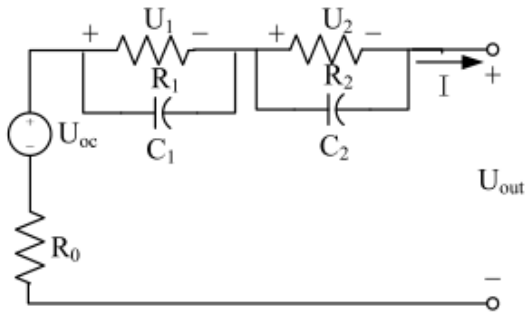

Figure 2-2: Two RC model (Fotouhi et al., 2016)

The data-driven framework is aimed at modeling the link between input and output signals from the battery. In the lack of in-depth battery knowledge, various data-driven frameworks, such as neural network models and support vector machine models (SVM), have been employed to simulate battery electric behaviors. A batteries data-driven model's success is dependent on both test data and training procedures (K. Liu et al., 2019).

2.4 Heat Generation of Battery

Battery is a complex electrochemical device which possesses non-linear behavior. Heat generation in battery is in both case of charging and discharging. It is incredibly significant to understand heat generation of battery because it has profound influence on its performance. Total heat is generated due to heat generation in the two electrodes, separator, current collectors, and tabs which are present inside cell (Lai et al., 2015). Energy equation for cylindrical cell was developed by Bernardi which contained electrochemical reactions, mixing effects, and joule heating. It has a direct influence on the temperature of the cell. According to (Peng et al., 2020) four types of heat are produced during operation of battery which are reaction heat (RH), side reaction heat (SRH), joule heat (JH), and polarization heat (PH). From various literature on basis of both theoretical and experimental understanding, it was found that heat

generation associated with battery is divided into reversible and irreversible heat. Overpotential resistance causes irreversible heat, while entropic change causes reversible heat.

$$Q = Q_{irr} + Q_{rev} = I * (V - U_{0uc}) + I * T\frac{\partial U_{0uc}}{\partial T}$$

where,

Q is total heat generated in the system,

Q_{irr} is the Irreversible heat due to potential,

Q_{rev} is the heat result from entropic change,

I is the total amount of current,

V is the open circuit voltage,

U_{0uc} is the loaded voltage and

T is the absolute temperature

The generation of reversible heat in cells occurs at cathode and anode. This is linked with entropy. Entropic heat originates from reversible entropy change during the electro-chemical reaction (Manikandan et al., 2017). The process is due to intercalation and deintercalation of electrons. This causes a change in the atomic arrangement due to which there are reversible heat changes in the cell (Choudhari et al., 2020). Entropic heat coefficient is a main parameter in this heat generation. It is a function of SOC. The entropic heat coefficient varies with the battery open-circuit voltage at varied temperatures. Heat generation of batteries during charging and discharging at varied currents and temperatures can be measured using calorimeters. The total heat generation of commercial 18650-type batteries was determined using an accelerated rate calorimeter, or ARC. From experiment analysis by (Manikandan et al., 2017), the entropic coefficient and temperature were shown to have a substantial association at various depths of discharge (DODs). It shows that reversible heat is considerable at lower temperatures. Increase in temperature of LIBs (Lithium-ion batteries) at low C rates is due to entropy changes in the electrode materials.

The Joule's heating of the battery cell is linked with change in potential drop in circuit. It is directly proportional to C-rate. Internal equivalent resistance consists of resistive, inductive, and capacitive circuits. Resistance is caused by the SEI layer, charge transfer, or diffusion in this case.

The figure below illustrates the heat in lithium-ion battery (Manikandan et al., 2017).

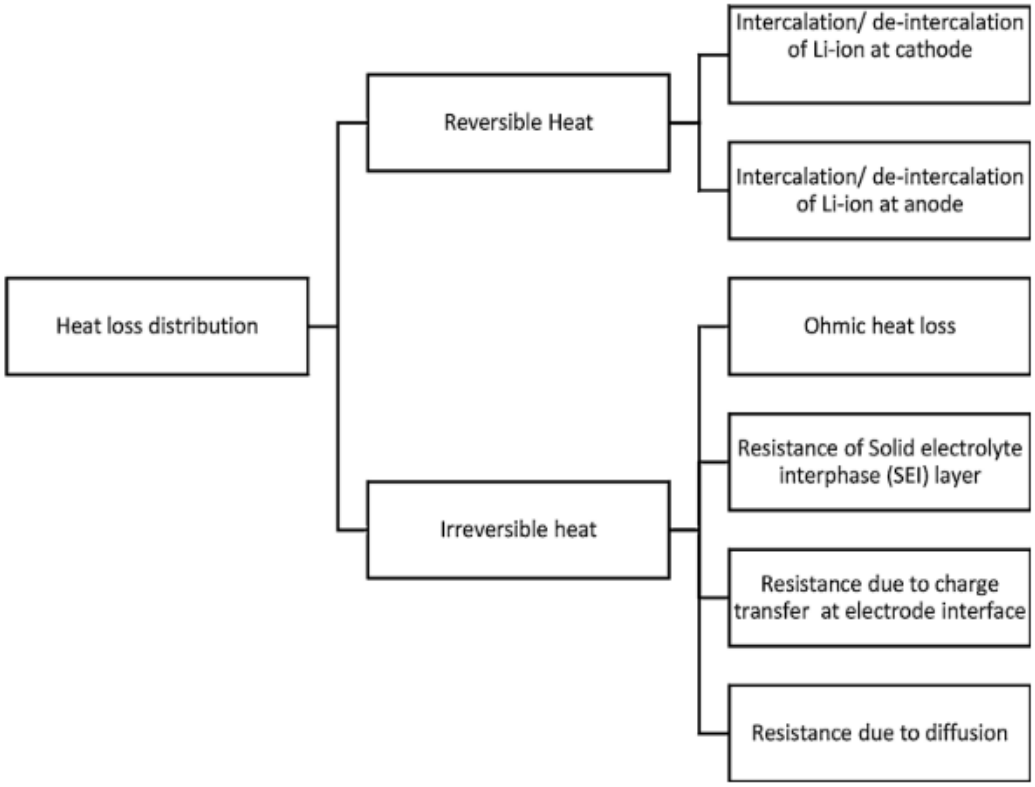

Figure 2-3: Heat generation in Li-ion model (Manikandan et al., 2017)

As the C rate increases, reversible heat decreases and becomes negligible at high C rate. The smaller value of reversible heat is mainly because both exothermic and endothermic reactions coexist for about the same length during the charging and discharging processes. So, there is balancing during both processes. Irreversible heat increases as current rate rises (C/2 to 2C) due to an increase in cell polarization, which is directly proportional to square of current (Manikandan et al., 2017).In (S. Liu et al., 2020), thermal analysis on 18650 LFP battery was conducted. Heat generation was evaluated at varied discharge capacities. There is greater electrical resistance due to ion migration and electron migration at lower temperature. Polarization and reactivity cause an abrupt increase in the total heat generation rate and exterior surface temperature of the battery during the final stage of discharge.

2.5 Temperature Effects

The characteristic of cell is affected in both cold and hot conditions working temperature. The heat generated by the battery pack in the charging/discharging process increases its temperature. The operating temperature and temperature variation within each cell can predict the working life of a Li-ion battery. Lithium-ion batteries can be

used in temperatures ranging from 20 °C to 60 °C at present. But 10°C to 40 °C is appropriate temperature interval (Li and Zhang 2020). The cell's temperature is mainly caused by heat generated within the cell during the charging and discharging states (K. H. Chen et al., 2017). The temperature variation among the cells should not increase 5 °C (Y. Zhao et al., 2019). At every 15 degrees increase in temperature there is decrease in 30 % of life cycle of cell (Amorim et al., 2022).Temperature regulation is regarded as one of the main problems in electric vehicles batteries.

There is an impact of low temperature on lithium-ion battery performance. It was extremely hard to charge a Li-ion cell at very low temperature. Lithium plating might tend to occur at high charging rates. Poor ionic conductivity of the electrolyte, strong polarization in the carbon anode, and high charge-transfer resistance on the electrolyte-electrode are some of causes of cell breakdown at low temperatures. As there is decrease of temperature below 10 °C, the power and energy of Li-ion batteries could be lowered. According to (Amorim et al., 2022), 11.5 Ah Li-ion cell experienced a capacity loss of 25% after only 40 cycles at a charge rate of 0.5 C at a low temperature of 10 °C.

Elevated temperatures also have a significant impact on the performance of battery. Under elevated temperature in various cycles, capacity of positive electrode materials tends to decrease. When the temperature is above 50 °C, the capacity declines. Batteries might start to self-discharge at that elevated temperature mainly due to surface species breakdown due to high electrical conductivity which increases the rate of self-discharge. When the temperature range is between 90 and 130 °C, then exothermic breakdown occurs. The negative electrode will start to react with organic electrolyte around 69 °C, producing combustion gas. At roughly 130 °C, melting of separator begins which allows short circuits between the electrodes. According to (Wu et al., 2021) ,aging mechanism and the state of health of lithium-ion batteries was found using incremental capacity (IC) analysis. It was found that when there is decrease in the ambient temperature, the IC peaks tend to move in regions of a lower voltage. As a result, it limits the charge-transfer dynamics due to an increase in polarization resistance at low temperatures.

According to the curve fitting analysis of this study, the lithium-ion battery's discharge capacity was approximated as a third-degree polynomial of temperature. The performance of very active electrolyte in the lithium-ion battery tends to decay as the temperature rises. Due to this, discharge capacity increases at beginning and finally

falls down. In interval of ambient temperature between 25 and 55 degrees Celsius, the discharge capacity of lithium-ion batteries is high. According to discharge efficiency and calculations of cycle life, the recommended operating temperature of a lithium-ion battery is 20-50 C. (Lu.et al ,2019) conducted an experiment to analyze the temperature dependency of lithium-ion batteries. It was found that when discharging temperature was reduced from 20 °C to 10 °C, discharging capacity was degraded at higher discharging rates. There was very less degradation in the temperature range of 20 °C to 40 °C calculated for all discharging rates which was evaluated during experiment. This finding gives us a hint that EV batteries should be kept at a temperature between 20 °C to 40 °C in order to reduce capacity and power degradation of cells at low ambient temperatures.

2.6 Battery Cooling

Many studies have been conducted in the past to solve the problem of maintaining temperature requirements of lithium-ion modules and packs.

In the paper (K. H. Chen et al., 2017), they examined air cooling architectures where two different cooling concepts, "channel design" as well as "fin design" cooling are investigated and concluded that air cooling needs much greater volumetric flow rate in order to achieve exact cooling performance as of liquid cooling. At natural convection, maximum value of temperature is 64.8 °C and minimum value of temperature is 57°C which is very higher than normal operating range (Behi et al., 2020).Also, they varied the gap between cells. By extending the gap between the cells up to 4 mm, the overall volume is simply increased, and subsequent flow path is not conductive to production of turbulence flow, lowering overall heat transfer coefficient. In terms of heat dissipation and overall volume, the spacing value of 2 mm is suitable for the 4 6 cylindrical battery modules. According to (Xie et al., 2017), three elements (air-inlet angle, outlet angle, and the gap between battery cells) are used to produce the orthogonal test table using the CFD approach to improve thermal performance. The best cooling performance is achieved at values of the air-inlet angle is 2.5°, the channel gap is identical, and the air-outlet angle is 2.5°.The application of PCM in the spaces between Li-ion cells reduced the temperature rise significantly. However, PCM's weak thermal conductivity might cause delayed heat escape to the environment, resulting in

full melting of the PCM during abusive battery use, resulting in an adverse thermal environment for the battery (Khateeb et al., 2005).

The carbon fibers are added to PCM for improving heat conductivity substantially (Samimi et al., 2016).Also, the carbon fiber mass ratio's impact on heat transfer was studied which improves the thermal conductivity of PCM.

According to (Shang et al., 2019), it's difficult for improving battery's total performance by focusing on a single aspect. The unit factor analysis as well as the orthogonal test are used to optimize factors for the thermal performance of the battery module (mass flow rate, input temperature, and the breadth of the cooling plate). When the input temperature is 18 °C, mass flow rate is 0.21 kg/s and the cooling plate width is 70 mm, the best cooling performance is achieved. In (Roe et al., 2022), the state-of-the-art about submerged cooling of lithium battery is discussed. Immersion cooling makes the system design simple, eliminates complex systems, and suppresses thermal runway. As a result, immersion cooling with dielectric fluid was determined to have the best cooling performance. However, certain drawbacks are there, such as the increased complexity/cost pertaining to condensing evaporated vapor and high viscous fluids creating high pumping losses. According to (Dubey et al., 2021),Immersion cooling's effectiveness in improving cell temperature, cell to cell temperature difference, cell temperature gradient, and module pressure drop is explored. Immersion-cooled battery modules perform substantially better than cold-plate-cooled battery modules due to the decreased density and viscosity of the investigated dielectric liquid.

According to (Zhou et al., 2022), by submerging lithium-ion cells in non-conductive coolant, a battery thermal management system with submerged cooling was developed. The electrical and thermal nature of cells were derived using the electric-thermal coupled model in ANSYS Fluent with the NTGK model. The MAT went up to 51.8 C when natural cooling was used, and 53.6 C when stationary submerged cooling was used. The MAT was decreased to 38.9 C by passing coolant at 1 mm/s and discharging at 3C, well inside the acceptable range of lithium-ion cells.

In the review paper (Lu et al., 2018), the technological advancement relevant to Lithium-Ion battery thermal safety issues are methodically and completely examined. The major discussion topics are thermal runaway modeling, behavior modeling and tests, and LIB pack safety management procedures. According to the paper for the behavior modeling and tests, pseudo-two-dimensional (P2D) model, being frequently used, strikes a fair balance between modeling performance and computing expense.

Furthermore, electro-thermal-chemical-coupled modeling techniques are presented for improving analysis precision while considering temperature-dependent aspects. For thermal runaway, both cell and system-level solutions for thermal runaway prevention have been briefed. Safety devices at the cell level, such as safety plugs, normal fuses, and separators, are widely used to manage cell hazards.

In the review paper (C. Liu et al., 2020), major focuses are on techniques and applications to enhance the overall thermal conductivity regarding PCM materials, as well as perspectives on the future of the material. The following results were obtained: The advantages of the passive battery thermal management systems include simple form and low production costs. When it comes to pricing, however, it can be tough to match the demands. In case of active battery thermal management system, employing metal fins to enhance the PCM thermal conductivity would considerably improve the system's heat dissipation capacity, it increases the system's weight and fabrication cost at some level. However, the approach of increasing fillers raises the heat dissipation capacity of PCM to a certain extent, and the vital work to gather related knowledge and fully comprehend mechanisms during the preliminary stage.

According to (Mokashi et al., 2020), To achieve the lowest maximum temperature of cell module, five different fluids are chosen and studied. Following that, conjugate heat transfer conditions were used. The flow of gas coolants across the pack generates a smaller decrement in maximum temperature because of poor thermal conductivity, and nanofluids aid to reduce temperature from certain critical threshold at moderate Reynolds number. In the paper (Kizilel et al., 2009), the advantages of adopting PCM battery thermal systems over traditional cooling systems are investigated. The following results are obtained: a PCM-graphite mixture absorbs then transfers heat fast. It is feasible to achieve uniform cell temperature for both normal and stressed settings by implementing passive battery thermal management system. The heat conduction and absorption properties of the PCM-graphite matrix avoid thermal runaway and guarantee safety in high stress circumstances. PCM technique is an effective and efficient alternative to air cooling for compact packs, and it considerably simplifies the cooling design for PHEVs.

According to (Y. Zhao et al., 2019), to give additional cooling capability for battery cooling, liquid cooling was integrated with copper foam/paraffin composite phase change material (CPCM). ANSYS FLUENT was used to create a three-dimensional system model of the BTMS for PCM and liquid cooling. The temperature

of module was around 25 °C after 1800s operation. There was no discernible temperature variation between the single cells. The surface temperature of the battery was lowered by 14 degrees Celsius.

According to (D. Chen et al., 2016), performance of single prismatic cell by direct air-inlet cooling, direct fluid cooling, indirect jacketed liquid cooling and cooling with fins were compared. An electrothermal-chemical battery modelling for a prismatic was created with the use ANSYS/Fluent. The findings revealed that air-conditioning systems require more energy than alternative systems to control at the exact temperature. The greatest temperature rise in an indirect liquid cooling system is the smallest. Similarly, fin cooling system increases 40% of cell's weight. Direct liquid cooling is less practicable than indirect cooling.(Y. Chen & Evans, 1996) developed and investigated behavior of prismatic lithium-ion battery cooling with mini channeled cold plates under varying loading conditions. Coolant velocity affects battery thermal performance most where maximum temperature and maximum temperature difference of battery and battery pack were around 40◦C and 5◦C. The main parameters used was only velocity where other parameters were not optimized.

In (Yang et al. 2019), they explained the chemistry of cell modules and evaluated dependency of battery parameters on temperature value as well as current rate. It has been discovered that battery temperature impact on those parameters is significant. Furthermore, it has been discovered that the drive cycle with intense power consumption develops heat quickly, resulting in potential difficulties such as danger, degradation, and damage.Less development of heat pipes, standards of production, equipment, and so on, the use in heat pipe battery thermal management is in the research phase and has not been explored (Wang et al., 2022).(Z. Yang et al., 2019) suggested a prismatic Li-ion cooling system based on liquid metals. The mathematical study along with numerical simulation demonstrated that liquid metal is an excellent coolant for use in the battery thermal management of batteries in EVs under stressful situations. The weight of battery cooling system is high if we use liquid metal cooling system.

According to (Zhou et al., 2022) increment in thermal conductivity of coolant lowers the temperature but has no considerable effect on temperature distribution. There are still certain technological issues to be addressed in the further work, such as extreme cooling and pricing of PCM, which is a major concern which can affect the performance and stability of PCMs and must be further explored and improved (C. Liu et al., 2020). According to (Zhao et al. 2019), the temperature variation of battery while

it is charging and discharging at different rates is the accurate and reliable datum for CFD simulation and analysis instead of certain value of heat flux. There are gaps in the research on lifetime, fluid behavior, material choice, sustainability, and the usage of immersion for battery safety (Dubey et al., 2021). According to (Chen et al. 2016), module level comparison of BTMS is needed to further understand the system efficiency.

2.7 Liquid Cooling

The liquid cooling systems and device give improved thermal as well as cooling efficiency. It is one of the most used methods of cooling batteries and is employed with direct or indirect contact interface between coolant and battery. Model S, Model 3, i3, and i8 from Tesla. The liquid cooling system and devices are used in the Chevy Volt. The serpentine channeled liquid cooling technique employed by the Tesla Model S is protected by patent (Kim et al., 2019). The cooling system faces challenges such as an increase in battery temperature, a rise in maximum battery temperature, and non-uniform temperature distribution across cells/modules/packs because of air's limited thermal heat dissipation rate and specific heat capacity (Deng et al., 2018).

The two types of liquid cooling systems are immersion cooling systems and cold plate-based systems. Cold plate liquid cooling is utilized in a wide range of performance required applications, like power storage, space transportation, electric vehicles, security, and non-residential power supply cooling, and even some overclocked computers. Submerged cooling is used in a few applications, including bitcoin mining, green file servers, and high-performance computing clusters (HPCC).

2.7.1 Cold Plate Cooling

A cold plate is a device that is used to keep an object cold. It is usually made up of a metal plate that is cooled by a refrigeration mechanism such as a chiller. This device has a wide range of uses and sectors, including air conditioners and refrigerators, food cooling, and medical applications (Coalition Brewing, 2020). Cold-plate liquid cooling devices can pass heat many times faster than forced air cooling. Since it does not rely on system airflow, a cold-plate system is more modular in its mechanical design and delivers higher performance cooling with a smaller system. Using liquid can replace bulky systems such as heat sinks, fans etc.

A 3D thermal system of a parallel flowing mini-channel coolant flowing cold plate liquid cooling system for rectangular LIBs. The homogeneous and isotropic nature of battery and aluminum was considered. According to this study, the maximum temperature decreases with an increase in the number of coolant flow channels and coolant mass flow rate (Huo et al., 2015).

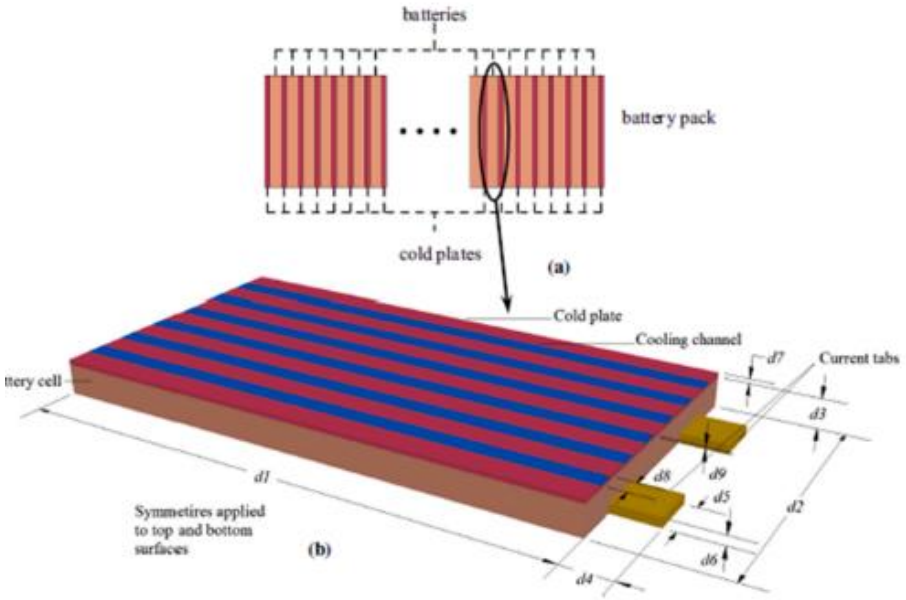

Figure 2-4: Parallel flow mini-channel (Y. Huo et al., 2015)

A small channeled cold plate TMS for LIBs was proposed and statistically explored (Rao et al., 2016). The impacts of channel number, intake mass inflow rate, direction of flow, and channel width for heat dissipation were investigated. A five-channel cold plate is enough for improving temperature behavior by the coolant flow rate increment.

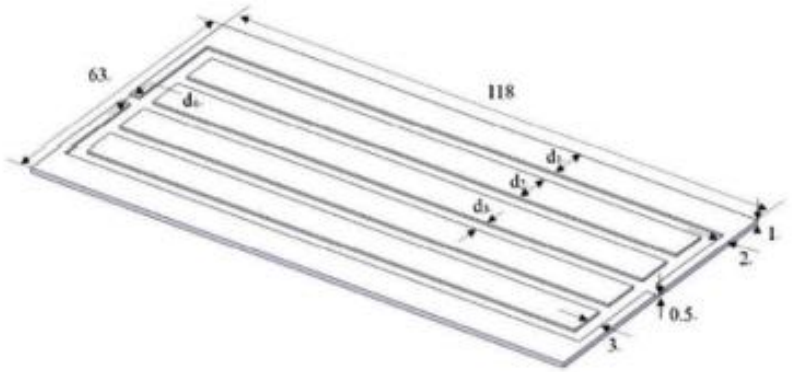

Figure 2-5: Mini channel cold plate(Rao et al., 2016)

The impacts of mass flow, number of cold plates, channel dispersion, and direction of coolant flow on thermal response of battery were explored for Serpentine type cold plate (Rao et al., 2016). A liquid cold plate battery pack of four rectangular lithium cells with five cold plates were created to evaluate the battery pack's thermal performance.

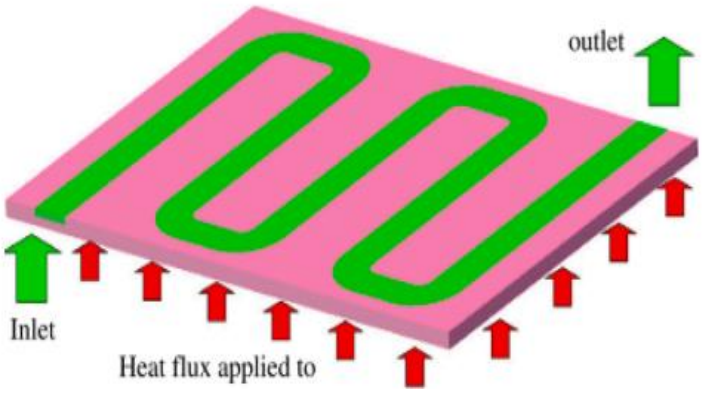

Figure 2-6: Serpentine cooling system(Rao et al., 2017)

Maximum temperature as well as maximum temperature dispersion are substantially below 35°C and 5°C, for a serpentine channel cold plate with coolant as ethylene glycol (Jiaqiang et al., 2018).

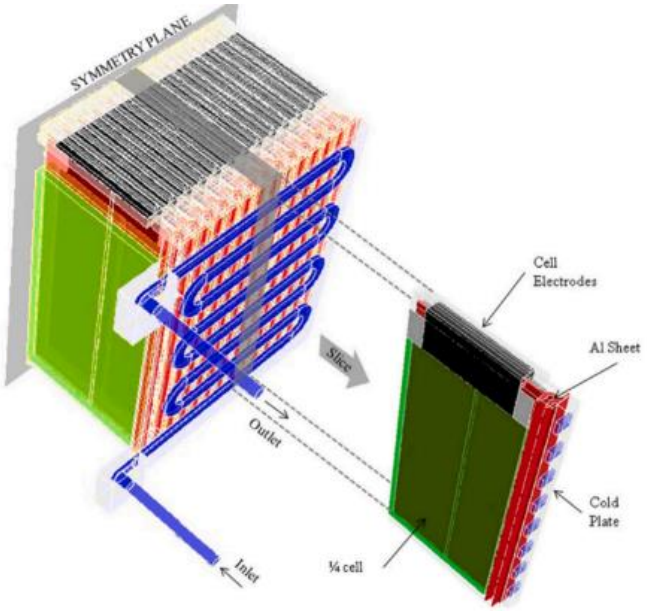

Figure 2-7: Serpentine cooling system (Jiaqiang et al., 2018)

Anthony Jarrett and colleagues built and computationally simulated the ability of a vortex-shaped liquid cold plate, as well as modified its design for improved energy efficiency (Jarrett & Kim, 2011).

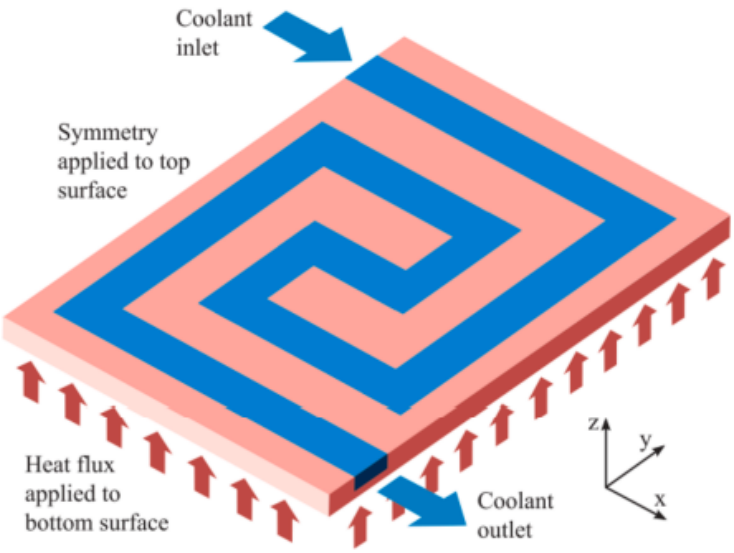

Figure 2-8: Vortex shaped cooling plate(Jarrett & Kim, 2011)

Meanwhile, researchers are investigating the impact of three characteristics (channel diameter, gap spacing, plate thickness) over the C-type cooling plate's maximum temperature, temperature differential, and pressure drop are being investigated. The cobweb type is more effective for decreasing the maximum temperature and temperature distribution of battery module (Q. Zhao et al., 2022).

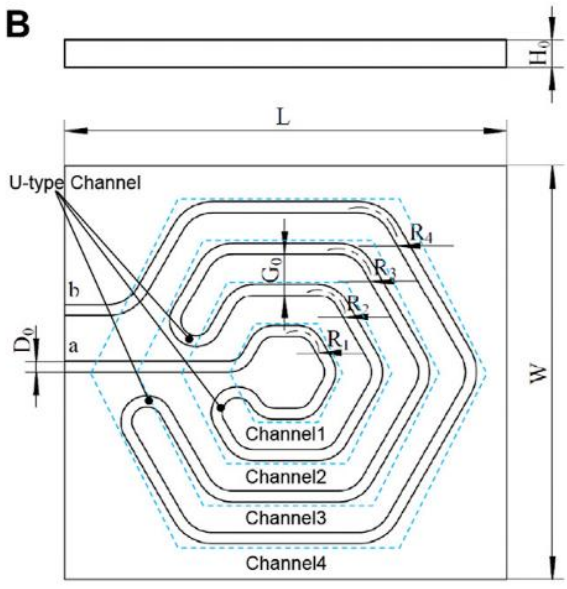

Figure 2-9: Cobweb type cold plate(Q. Zhao et al., 2022)

From the literature, we know that cooling system optimized on numbers of parameters, but they were very different from one another and had different boundary condition and thermal loading.

2.8 Air Cooling

2.8.1 Unit Cell Module Cooling

To achieve the necessary voltage and capacity, cylindrical lithium-ion cell modules are arranged in series and parallel configurations. In order to safeguard the system from atmospheric conditions in practice, the components are always air proof and waterproof. Standard terminology for this process is ingress protection. A variety of air conditioning techniques are very useful for cooling the battery module, but none of them take the battery module's ingress protection into account. In most cases, air is passed directly through cells for analysis and experimental validation. (Xie et al., 2017).

2.8.2 Module Air Cooling

Air cooling is the most natural method of battery cooling. There are two types: free and forced type cooling. These systems are straightforward, cheap, electrically safe, small, leak-free, and require little maintenance. Natural cooling was found to be insufficient to fulfill the needs of an elevated temperature environment, larger battery pack thermal management systems, and greater charge-discharge cycles. Forced-air cooling is employed to circumvent these limits, along with the installation of fans, developed air-flowing channels, fin structures, and so on (Tete et al., 2021). A continuous flow of air is supplied from the outside of the driving EV at battery systems, dissipating heat created inside the pack. In natural air-cooled BTMSs, several research techniques like geometric structural optimization and parametric system development are applied.

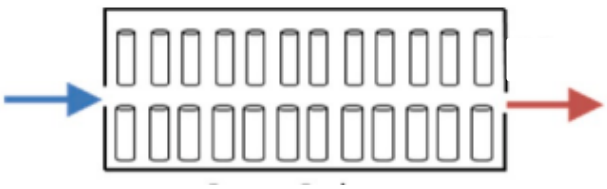

Figure 2-10: Passive air-cooling system

Force air cooling uses a constant flow of air from an additional blower to eradicate heat from battery pack. Several air-cooled BTMS optimization strategies, such as fan positions optimization and operating timing of cooling fans to monitor the amount of extra energy pulled from cells to limit heat development in the pack. The

organization of individual objects in modules, novel air flow designs, and improvement of air channel configurations have been the area of recent development and research on air-cooled systems of heat dissipation.

The forward cell in series ventilation is near to the air intake, has a high flow rate, and a low temperature. Because battery is close to the air exit, its heat transfer efficiency is reduced, and the temperature is increased. As a result, the temperature consistency of the battery module is poor. Air travels through the battery faces simultaneously during parallel ventilation. The air velocity as well as airflow are very uniform across battery faces. The heat transfer on each battery face is identical, and battery module's temperature uniformity is improved. Parallel ventilation is a prominent heat dissipation approach for air-cooled batteries in thermal management systems for these reasons(Wang et al., 2022).

CHAPTER THREE: METHODOLOGY

3.1 General Methodology

The project's literature review was done over the course of the project. Heat generation was calculated after the appropriate lithium-ion cell for the study had been selected.

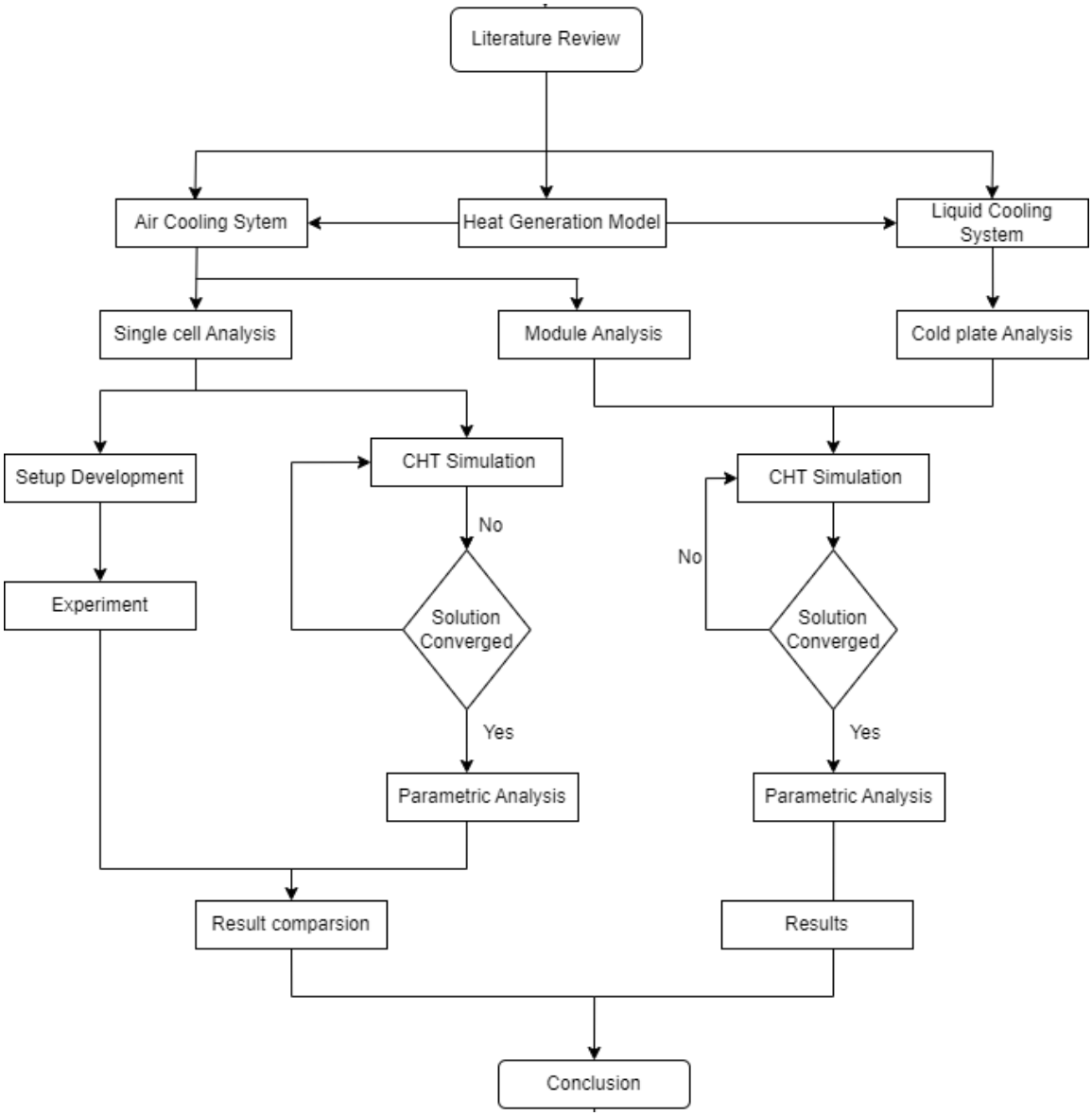

Figure 3-1: Flowchart of methodology

The unit cell module was subjected to CAD modeling and CHT analysis. Response Surface Optimization was also performed on the candidate points. The results were compared to the experimental data. Using this as a validation to the analysis procedure, the 3S3P module was developed and analyzed for cooling strategies. Response surface analysis was used to parametrically analyze air cooling and cold plate

configurations. The final documentation completed our project. Figure 1 depicts a flowchart of our project's methodology.

3.2 Heat Generation

For irreversible heat, internal resistance was calculated, and Joule's heating was used for heat generation. There were numerous critical procedures involved in determining a lithium-ion cell's internal resistance. Firstly, the battery was fully discharged and allowed to stabilize.

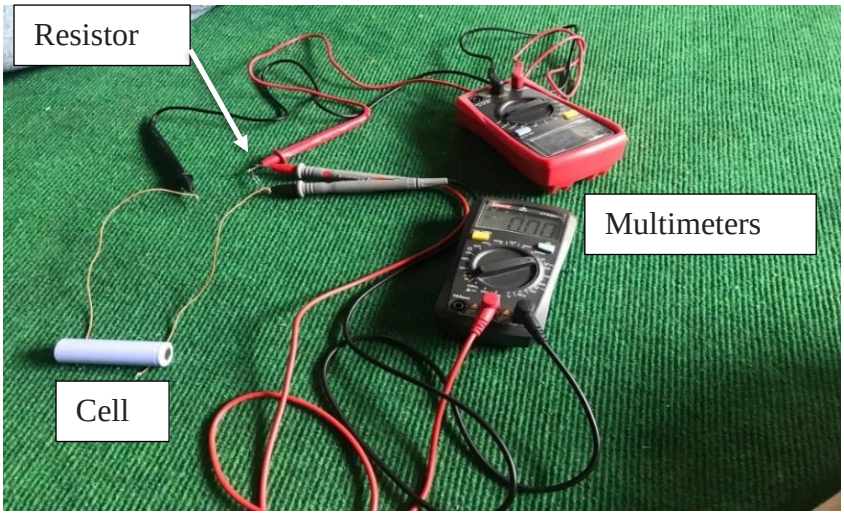

Figure 3-2: Heat generation measurement setup

The next step was to choose external resistance and a multimeter with a battery test feature. The positive and negative battery connections of the test apparatus were then safely linked. The Open Circuit voltage was measured along with the resistance.

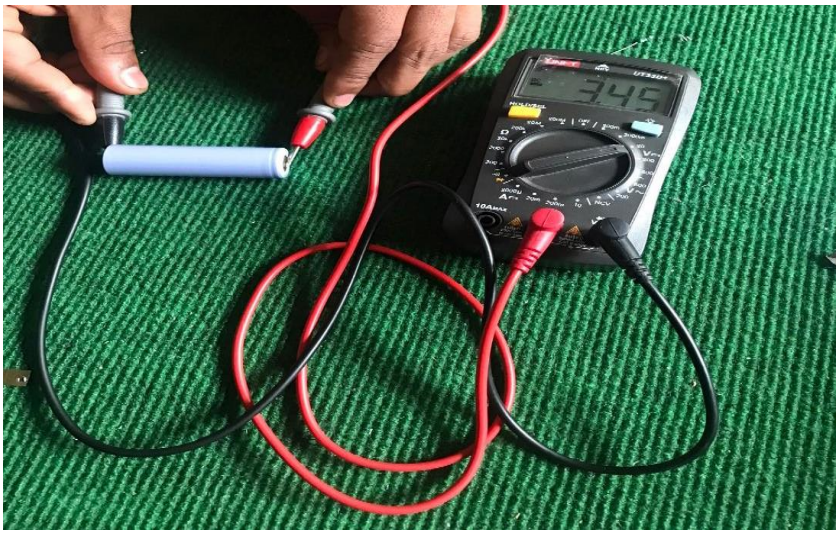

Figure 3-3: Open circuit voltage measurement

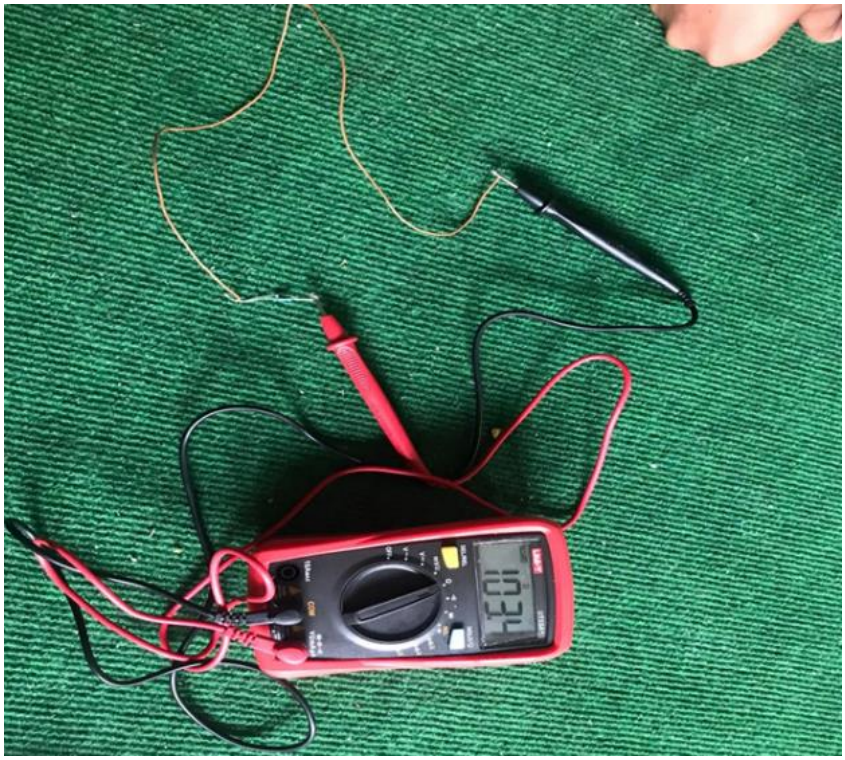

Figure 3-4: Measurements of resistance

The test apparatus delivered a known current to the battery and measured the voltage across the cell as a result. This made it possible to apply Ohm's law to compute the cell's internal resistance. The test's outcomes were analyzed to reveal information about the battery's power output and heat generation.

Figure 3-5: Measurement for loaded current and voltage.

According to (Lu et al., 2019),the calculation of various parameters is based on formula given below:

Internal resistance of the cell *(r)* = $\frac{O_{CV}-V}{I_r}$

Joule's Heat (Q_j) = $E * I - I^2 \cdot r$

Entropy Heat (Q_r) = $I * T \cdot \frac{dV}{dT}$

Total heat *(Q)* = $Q_j + Q_r = E * I - I^2 \cdot r + I * T \cdot \frac{dV}{dT}$

where,

O_{cv} is open circuit voltage,

V is loaded voltage,

I is current flow through a circuit,

T is an absolute temperature and

E is the emf of cell.

3.3 Battery Module and Ingress Protection

A cell, which is the basic component of a battery, is made up of an anode, a cathode, and an electrolyte. As a cell is charged, ions move through the electrolyte from the anode to the cathode, and when the cell is discharged, they move in the reverse direction. A module is a group of cells that have been linked in parallel or series to increase the battery's voltage or capacity.

Ingress protection, or IP rating, is a standardized method of measuring how well enclosures operate to keep solids (such as dust) and liquids out. An IP rating for a battery pack represents the level of protection provided by the battery pack's casing against dirt, water, and other potential hazards. A higher IP rating indicates more reliability. A battery pack with an IP68 certification is resistant to dust and water immersion up to 1.5 meters, whereas a battery pack with an IP67 rating is resistant to both. When selecting a battery pack for a certain application, consider the IP rating because the environment in which it will be used might have a considerable impact on its performance and lifespan. The battery module we have developed was unit cell module and aluminum container covered with polyamide tape was used to exercise the ingress protection.

Figure 3-6: Aluminum container

3.4 Battery Thermal Management Systems

A battery pack is a collection of cells organized in various configurations. The electrochemical process of power generation, which is temperature, soc and environment dependent, determines battery performance (Tete et al., 2021b). The external environment and heat emitted from a chemical reaction caused by constant charging and discharging have a substantial impact on the change in temperature of the battery pack. Since the Lithium-ion battery is very sensitive to temperature, the battery pack must be kept at a consistent temperature. As a result, one of the most important functions of thermal management system is to control a desirable operating temperature range and uniform temperature field within the cell under adverse external conditions and throughout heavy charge and discharge cycles (Kim et al., 2019).The battery thermal management system should have characteristics such as robustness, lightweight, cheap cost, ease of maintenance, and consumption of less parasitic power. To keep a load at proper temperature value by decreasing heat at hot areas and supplying heat in cold climates is the major need of BTMS (Pesaran et al., 1999).There exist various types of battery temperature control systems, that are distinguished by the

power consumption, heat exchange medium, and interface of the coolant with the cell surface. Within this foundation, we examined the traditional type BTMS, such as forced air-cooling systems, liquid cooling systems (Tete et al., 2021b).

3.5 Conjugate Heat Transfer Simulation

The heat transfer analysis that involves simultaneous heat transfer between solid and fluid domain is Conjugate Heat Transfer. This kind of heat transfer incorporates convective and conductive heat exchange. Here, fluid, and solid are modeled as separate domains and interaction between the two are analyzed. The main goal of CHT is to analyze temperature distribution and heat transfer between fluid and solid domain which is by combined mechanism of heat transfer.

The general process of CHT Simulation is presented below:

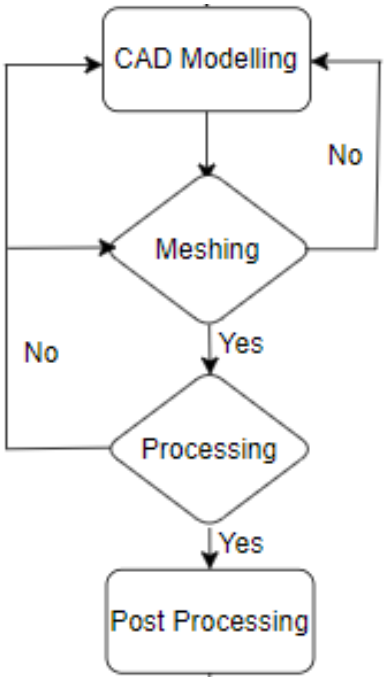

Figure 3-7: Flowchart of CHT simulation

The analysis is Steady State and 3D Analysis. Battery discharge is inherently transient. But certain applications could benefit from steady state with good accuracy. For an example, If the thermal time constant is significantly smaller than the discharge period, batteries can attain quasi-stationary state, and the steady state solution provides very precise results. Energy and user scalar equations are solved only for thermal simulations. Flow equation is solved in the air-cooling simulation of module. ANSYS Fluent 2022 battery model CHT Coupling has been used for the analysis.

Table 3-1:Cooling System Parameters

S. N	Inputs	Outputs
1	Tab current	Cell Average static temperature
2	Cell Power generation rate	Temperature distribution
3	Ambient Temperature	Inlet Pressure
4	Coolant Velocities	
5	Outlet Pressure	

3.6 Parametric Analysis

Parametric Analysis is the process of analyzing the parameters and their relationships with one another deducing the reasons behind the behavior of each parameter. We have attempted to perform parametric analysis using Ansys Design Exploration toolbox named Response Surface Analysis.

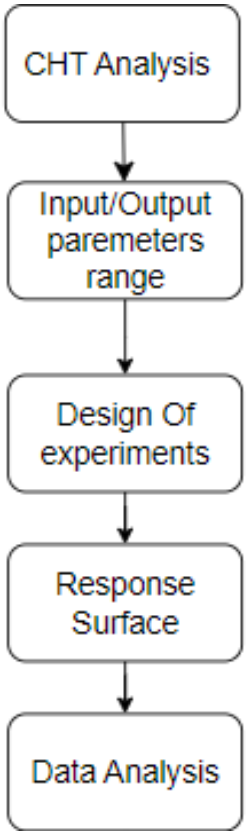

Figure 3-8: Flowchart of parametric analysis

3.6.1 Design of Experiments

Design of Experiment is a statistical method for design and analysis of experiments. In order to efficiently sample a design space and build a statistical model to forecast response, DOE is used. To plan an experiment using DOE, one or more independent

variables must be changed, and the impact on one or more dependent variables must be evaluated. Its objective is to establish the relationship between the independent and dependent variables.

- Here input parameters are geometry, flow velocity etc. which are defined in bounded range or at point.
- The output parameter is cell average temperature.
- In design point, high, low, and mid-point input value are used to extract the response which is sample data for number of experiments to be conducted.
- Then under design experiment type sparse grid initialization is used to extract other values from the given value of 3 data point.

3.6.2 Response Surface

A group of statistical and mathematical methods known as response surface approximations were initially developed for optimizing processes. A functional relationship between an output variable and a collection of input variables is sought by the response surface. Metamodel sparse grids use fewer parameters than other grid-based techniques which makes this method appealing for the numerical solution of moderate- and higher-dimensional problems. The equation below is the second order system with two independent variables for approximating the response surface.

$$y = \beta_0 + \sum_{i=1}^{k} \beta_1 x_i + \sum_{i=1}^{k} \beta_{ii} x_i^2 + \sum_{i<J} \beta_{ij} x_{ij} + \varepsilon$$

Here, x, y are variables and β are coefficients which can be found using the least square method.

The general flow for response is:

- In our numerical study we use spare grid as response surface type which is metamodel.
- Input parameters with geometry, flow variable.
- Output parameter temperature.
- Response chart for graphical representation.

3.6.3 Data Analysis

Graphical representation of response surface and input variables. This is given by a response graph. Building a statistical model to explain the connection between the factors and the output variable is a step in the response surface methodology (RSM)

data analysis process. Data analysis process is obtained after design of experiment and response surface.

3.7 Experimental Setup

We conducted an experiment for unit module air cooling system to observe heat production of a lithium-ion cell responding to air cooling at varying air inlet velocities while being rated ingress protection index. There are assumptions for the setup development. The fan was operated at three different velocities only. Normal air velocity is 0.2m/s (Hui Zhang, 2013) in room. Two thermometers were assumed to be enough to approximate the cell average temperature. The behavior of a cell was assumed to be same at 0.85C rate discharge or charge rate. Wood was used to approximate the gap between cell and aluminum thickness, filled with polyamide tape, wood, paper and thermal sensors. Based on the above assumptions, the setup was developed for analysis.

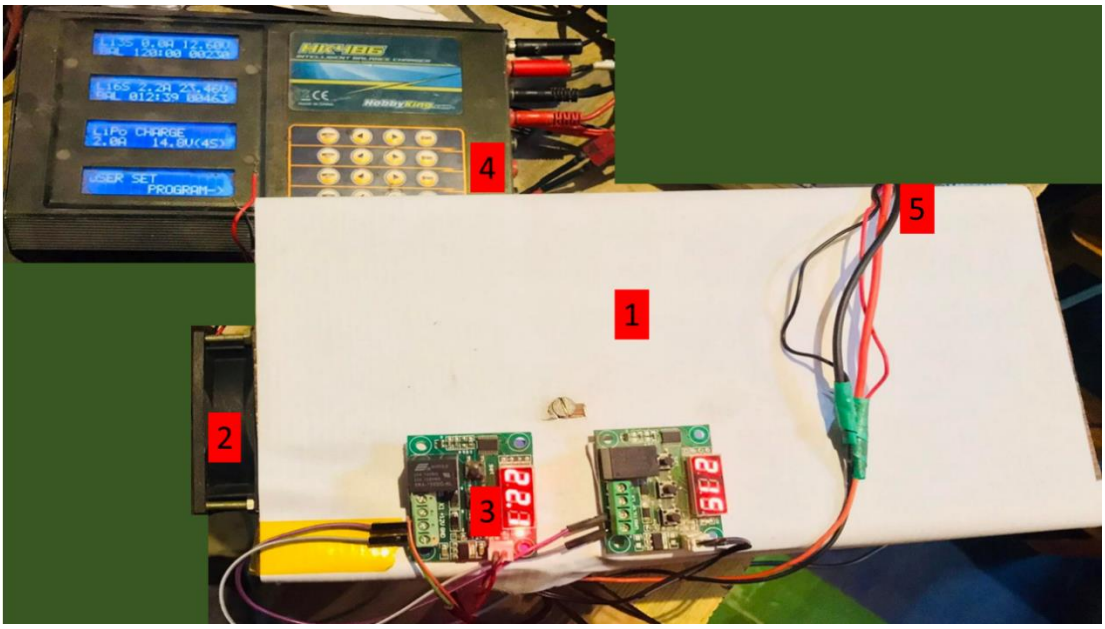

Figure 3-9: Experimental setup

For conducting our experiment, we have connected wire from negative and positive tab to charge-discharge module and temperature of cell is given by display of thermocouple temperature controller. Lithium-ion cells were used with nickel strip as busbar in both terminals of cell. That is covered by Kapton tape which acts as a good

electrical insulator. Here the process takes place at 0.85C rate. Our experimental setup composed of following:

Table 3-2: Different components used in setup.

S. N	Component's name
1)	Flow channel
2)	Fan
3)	Data logger
4)	Charging & Discharging equipment
5)	Connecting wires
6)	Li-ion cell
7)	Temperature sensor

Figure 3-10: Lithium-ion cell

Figure 3-11: Temperature sensor

The cell was charged at rate of varying current inputs and with time the current was measured along with the average temperature approximated using two temperature sensors housed inside the aluminum container.

3.8 Unit Cell Module Cooling

Ansys design modeler was used to create a CAD model for a battery cell experiment. First, the specifications and volume of the battery cell were determined based on the experiment's requirements. The software was used to design a 3D model of the cell, including the aluminum case, nickel electrodes, air domains, and any other components required for the experiment. The model was then refined and optimized to ensure that it accurately reflected the physical characteristics of the battery experiment while also being easily fabricated using workshop tools or other manufacturing

techniques. Overall, designing a CAD model for a battery cell experiment required careful consideration of the size, shape, and experiment components. The design parameters which can affect the “Average Cell Temperature” of the system are listed below:

Table 3-3: Parameters

S. N	Parameters
1.	Flow Channel Sizing
2	Module Placement distance
3	Ambient Temperature
4	Air inlet velocity
5	Aluminum thickness

Following assumptions have been made to simplify the analysis of our system based on literature and fabrication constraints, the CAD model is drawn using Ansys Design Modeler.

Table 3-4:Geometric assumptions

S. N	Components	Assumption	Reasons
1	Flow channel size	10cm*10cm*30cm	Available fan size
2	Module Placement	10cm from the fan	Fully developed flow reaches there.
3	Aluminum Shell thickness	0.8mm	Market Availability

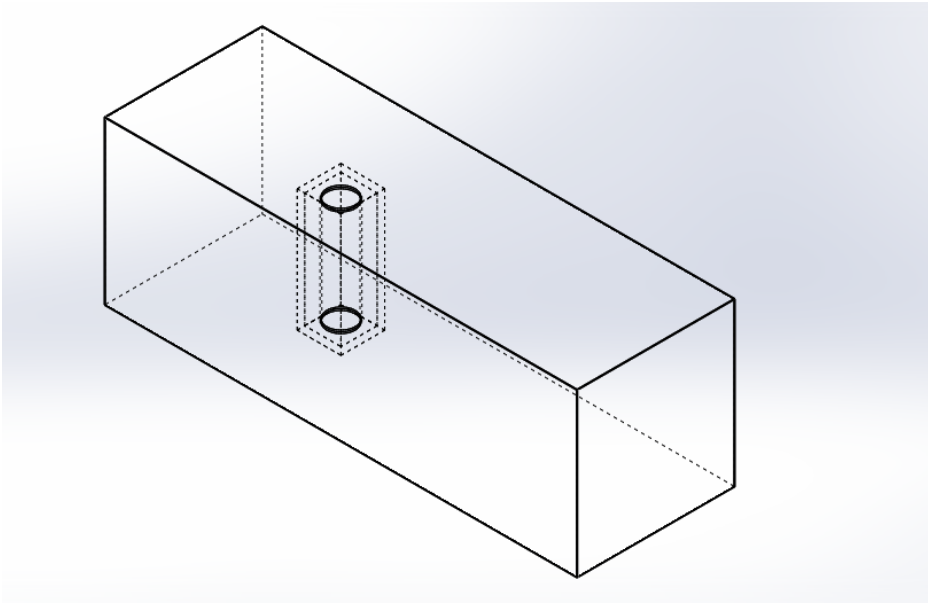

Figure 3-12: Isometric view of unit cell module

The Cad model is then meshed using watertight workflow in Ansys Fluent 2022 R1.

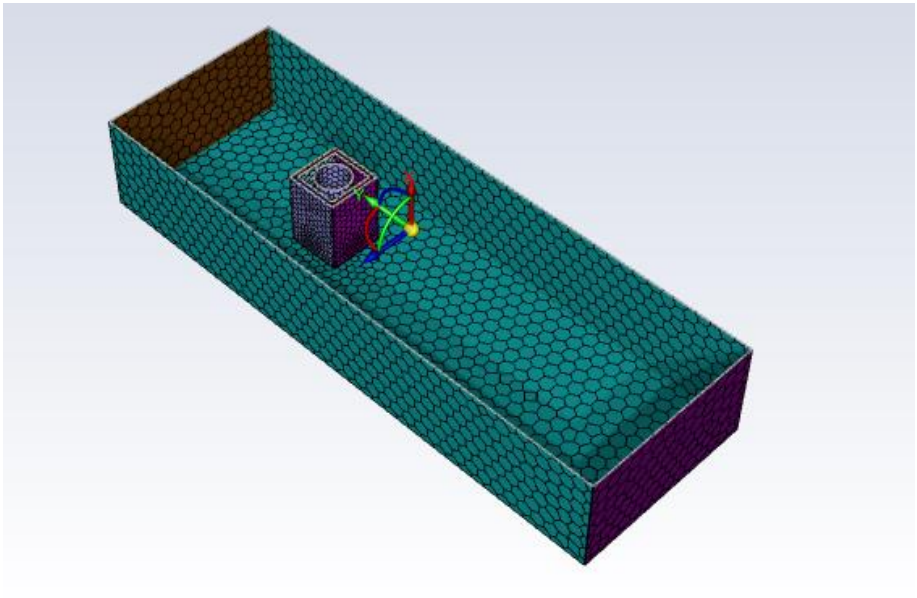

Figure 3-13: Surface meshing of unit cell modelling

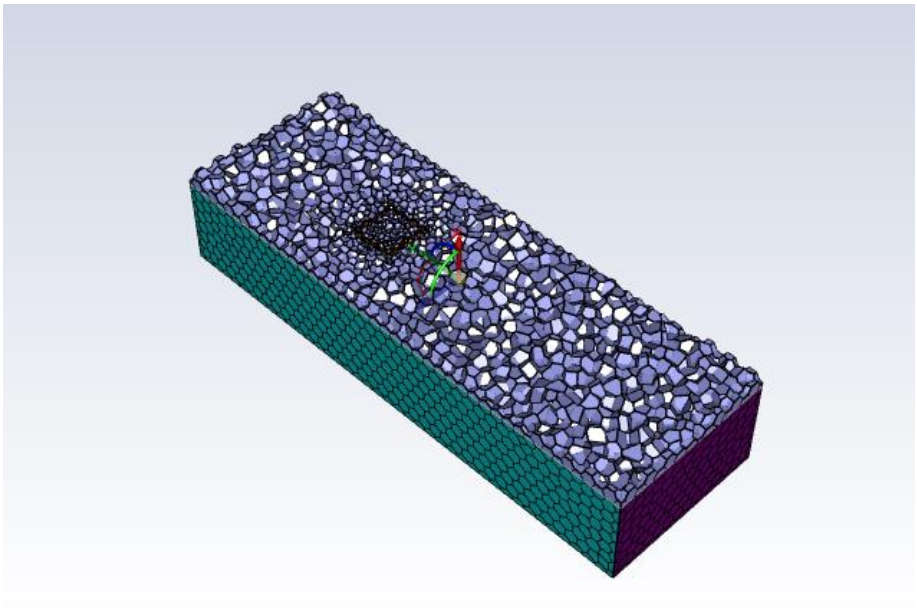

Figure 3-14: Volumetric mesh of unit cell

Volume mesh is generated from the surface mesh. The mesh is subjected to Ansys Fluent 2022 R1 to battery model for observing heat generation and temperature variation with air cooling.

3.9 Module Cold Plate Cooling

3.9.1 Cold Plate Cooling

Different methods of cold plate systems are simulated under different geometric configurations under different coolant velocities under constant cell spacing. The curve of cell average temperature vs velocity was obtained. Various configurations of cold plate cooling such as parallel, serpentine, vortex and cobweb were performed under different velocities. To obtain performance parameters of cooling plates cooling which are cell average temperature, surface temperature distribution and pressure difference between inlet and outlet, other parameters of cold plate such as cooling channel numbers and configurations are preserved as presented literature.

Table 3-5: General assumptions for cold plate design

Parameters	Values
Aluminum Cold Plate Thickness	10mm
Channel Path	6mm*6mm

Four diverse types of cold plates are derived from literature to compare the performance of cold plate cooling. Since the cold plates in the literatures are not comparable to each other due to different boundary conditions and size requirements standard module development was done to analyze cold plate performances. The 3D CAD model of each kind of design is done in the ANSYS Design Modeler. Detailed and well-defined geometrical drawings are in appendices.

3.9.2 Module Development

For the analysis of different cooling configurations, a 3S3P module is developed. The cylindrical lithium batteries are the most used type today(Prismatic Battery Cell and Cylindrical Battery Cell? How to Choose Between Them, 2019).3S3P module is developed and designed for the analysis. More than 3S3P module increase the analysis domain; less than that will not capture the dynamics of module. The aligned battery pack is optimal at cooling effectiveness as well as temperature homogeneity than staggered type arrangement, and finally, an artificial air cooling BTMS was installed for cross pack (Fan et al., 2019), but dynamics of battery cooling can be assumed to be similar. For battery pack with straight and staggered arrangements, the

necessary transverse cell to cell gap is 34 mm (Yang et al., 2015). The Supporting structure for the battery cells does not have much impact on the cell temperature. According to the findings, the thermal hotspot at cell is localized at the electrode as opposed to the entire battery. This unequal temperature distribution results in temperature non-uniformity, which reduces the cell life cycle and overall cell performance (Y. Yang et al., 2013). The cell to wall spacing is assumed to be 5mm, but it can be varied. The Insulation layer thickness and thickness of busbars is assumed to be 1mm. Using one cold plate on one face is enough to compare cooling plates. The module is modelled using nine 18650 lithium-ion cells based on the above assumption. The CAD modelling is done for the analysis.

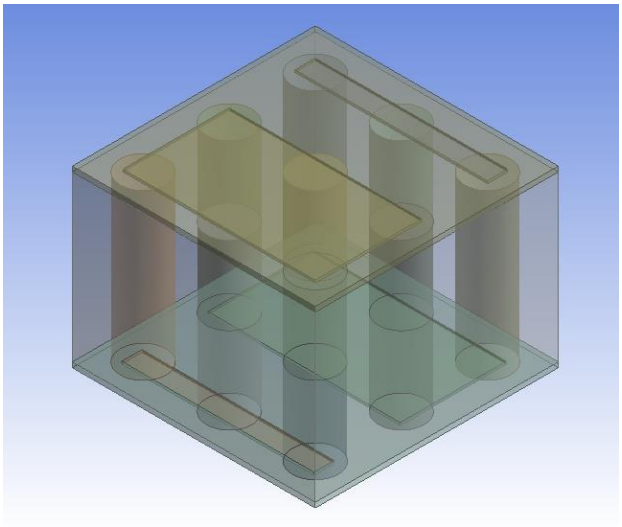

Figure 3-15: Standard 3S3P module

It consists of different parts cells, busbars, insulation, and internal air domain. Polyhedral meshing was done for the system using watertight workflow geometry in

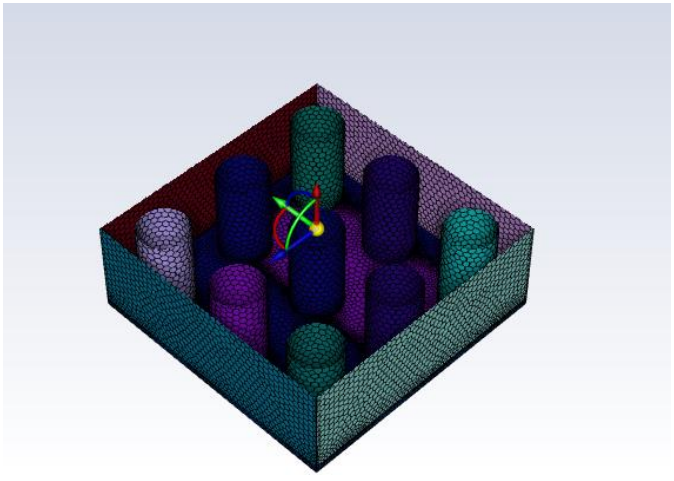

Figure 3-16: Module surface mesh

Ansys fluent 2022 R1 to observe the behavior of cell at ambient temperature air velocity of 0.05m/s is subjected to approximate air movement inside the air domain.

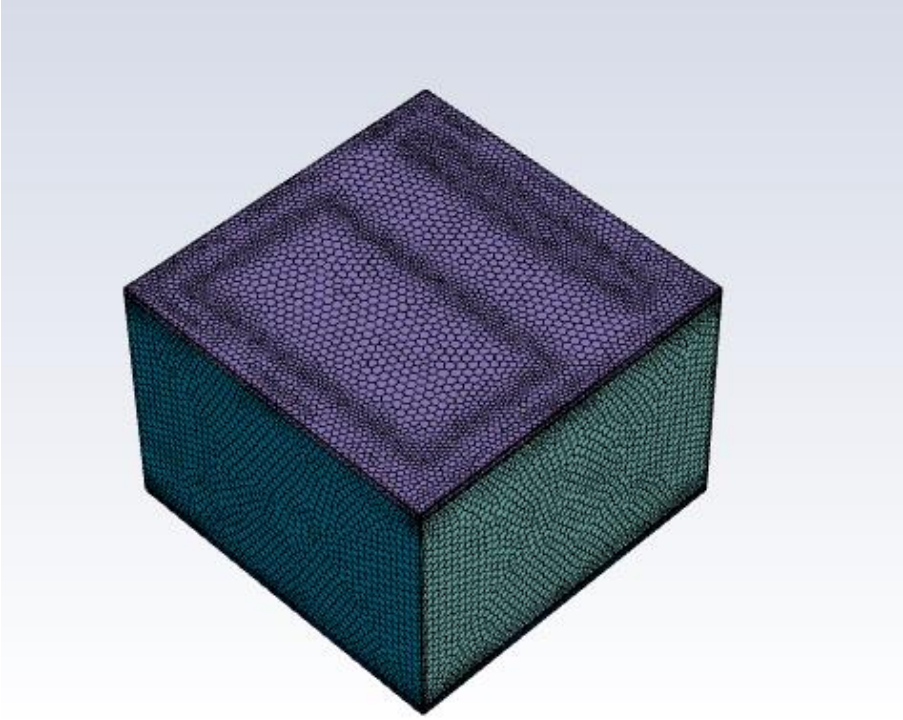

Figure 3-17: Module volume mesh

After the mesh generation is completed. The mesh is checked to ensure skewness lies below 0.85. The mesh file is subjected to processing stage.

3.9.3 CAD Modelling

Four different types of cold plates are derived from literature to compare the performance of cold plate cooling. Since the cold plates in the literatures are not comparable to each other due to different boundary conditions and size requirements standard module development was done in order to analyze cold plate performances. The 3D cad model of each kind of design is done in the Ansys design modeler.

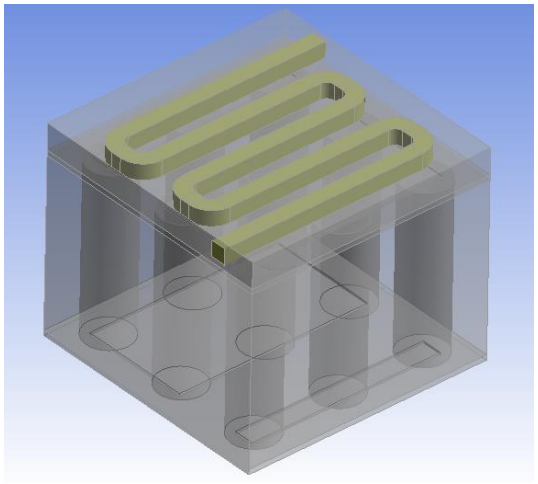

Figure 3-18: Serpentine type cold plate

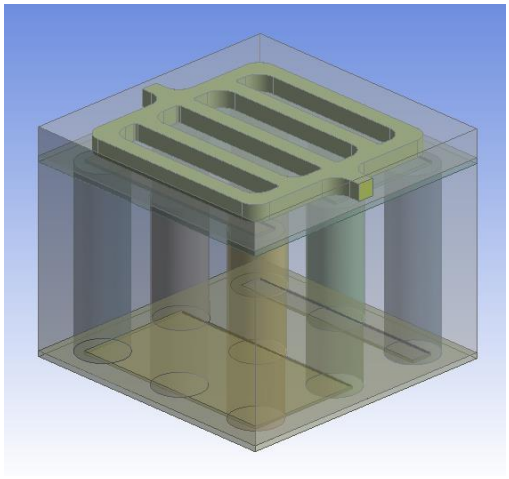

Figure 3-19: Parallel type cold plate

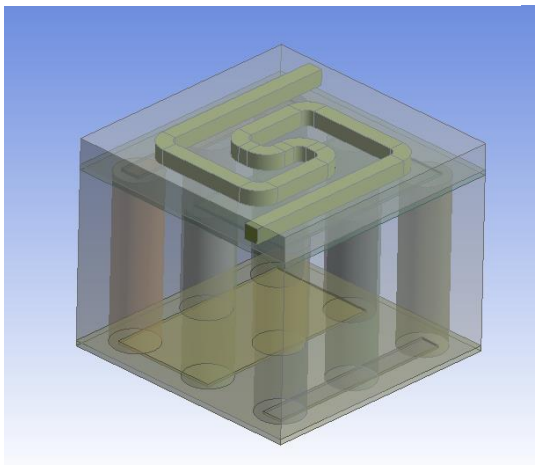

Figure 3-20: Vortex type cold plate

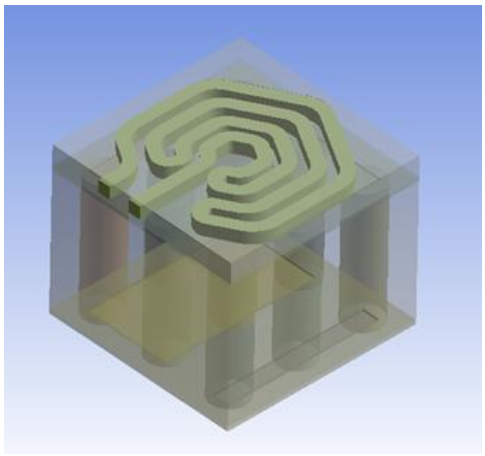

Figure 3-21: Cobweb type cold plate

Detailed dimensions of each type are in the appendix.

3.9.4 Mesh Generation

Conjugate Heat Transfer makes use of polyhedrons. Polyhedrons are presented to use the advantages of hexahedrons and tetrahedrons (rapid semi-automatic generation) while avoiding the disadvantages of both mesh types. The fundamental advantage of the polyhedral meshing method is that each cell has numerous neighbors, which allows gradients to be approximated accurately. Polyhedrons do not stretch like tetrahedrons, resulting in higher mesh quality and good numerical stability. Also, numerical diffusion gets reduced because of mass interchange across numerous faces. This yields a more precise solution with a lower number of cells. Ansys fluent watertight workflow is used to generate polyhedral mesh in each case. The quality of each mesh is checked for skewness less than 0.85.

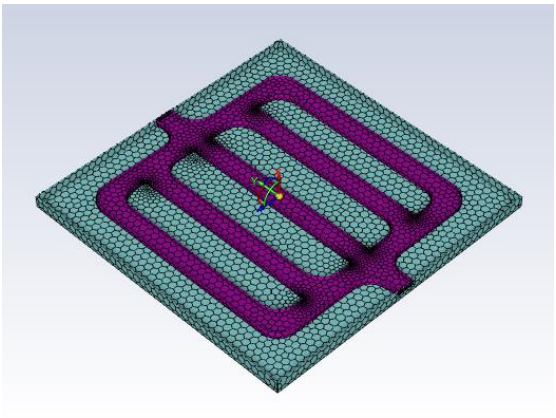

Figure 3-22: Parallel type surface mesh

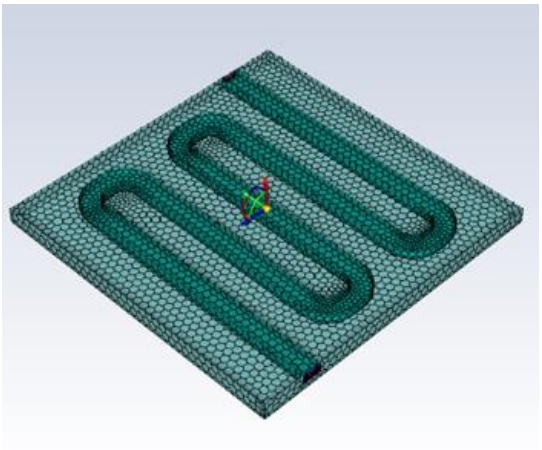

Figure 3-23: Serpentine type surface mesh

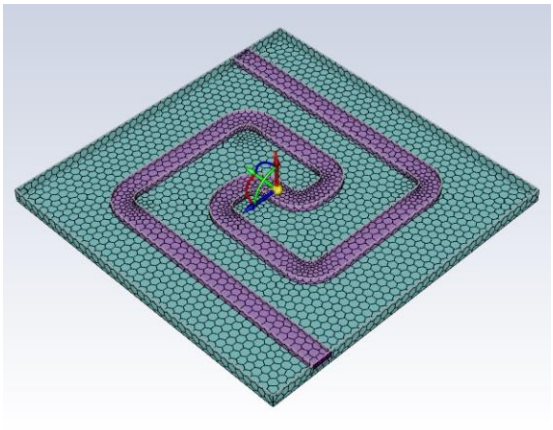

Figure 3-24: Vortex type surface mesh

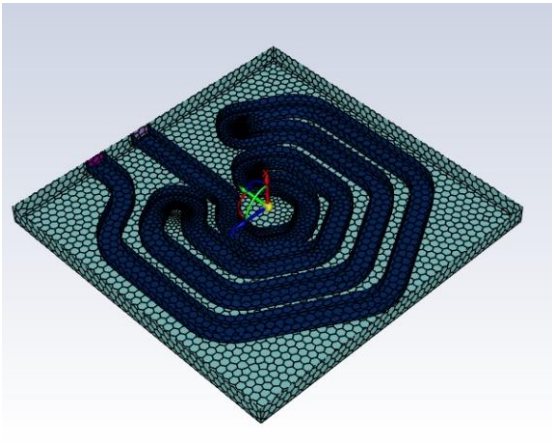

Figure 3-25: Cobweb type surface mesh

Ansys fluent watertight workflow is used to generate polyhedral mesh in each case. The quality of each mesh is checked for skewness less than 0.85. Numerous iterations are

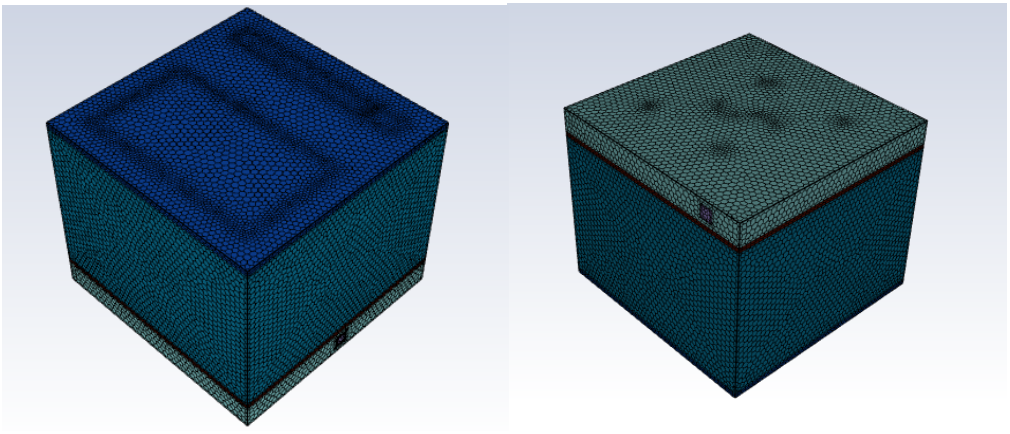

Figure 3-26: Volumetric mesh

done in order to improve mesh quality in each case. After the surface mesh is generated,

the body is subjected to volume mesh generation. This mesh is subjected to analysis in Ansys fluent 2022 R1.

3.10 Module Air Cooling

. Various configurations of 3S3P battery pack such as U shaped, Z-shaped, Single Input Double output and Single input Single output air cooling was performed under different velocities at constant cell spacing and curve of cell average temperature vs velocity was obtained

3.10.1 Module Development and CAD Modelling

The parameters varied in the analysis of air-cooling system are velocity and air flow configurations. For battery packs in alignment and staggered arrays, the necessary transverse distance is approximately 34 mm (N. Yang et al., 2015). Standard cell of 18650 of 3S3P combination CAD model is built in solidworks 2022 and exported in parasolid format in Design Modular of ANSYS. The geometry of the different air flow channel is shown in the figure:

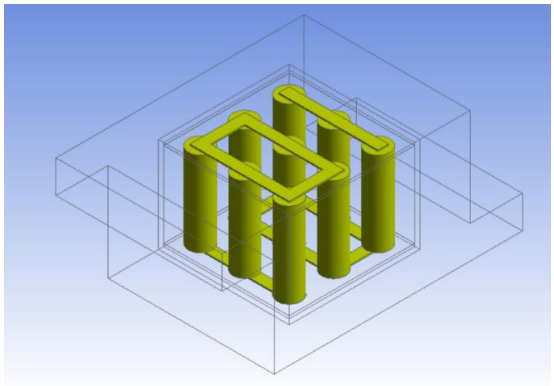

Figure 3-27: Z shaped geometry

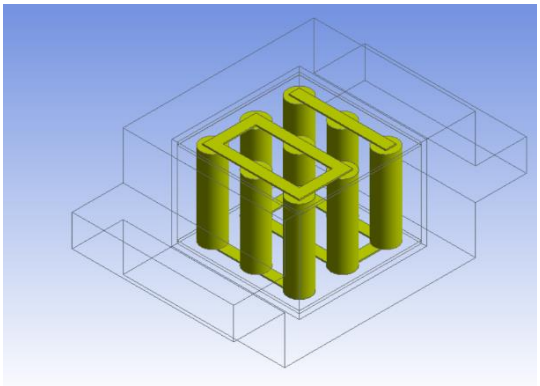

Figure 3-28: SISO geometry

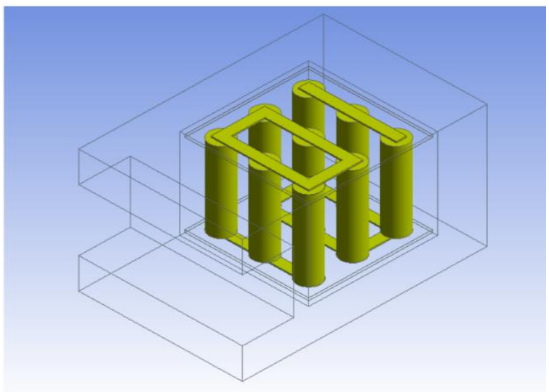

Figure 3-29: U shaped geometry

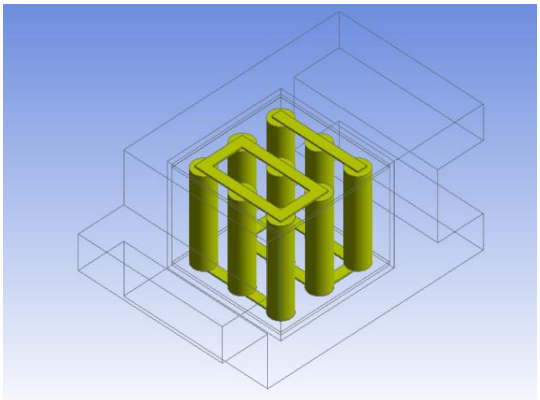

Figure 3-30: SIDO geometry

3.10.2 Mesh Generation

The geometry of elements is polyhedral in the mesh generation. The main advantage of polyhedral mesh is that every cell has numerous neighbors, which allows gradients to be well approximated. Polyhedrons are additionally less prone to stretching than tetrahedrons, resulting in increased mesh quality and numerical stability of the model. The mesh of different configuration can be observed in the figures below.

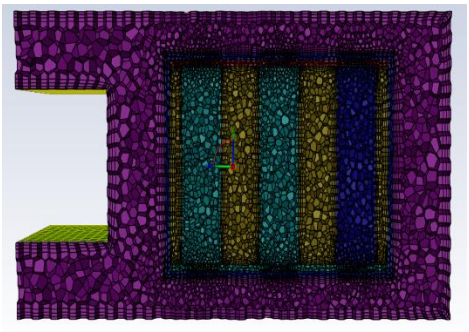

Figure 3-31: U shaped mesh

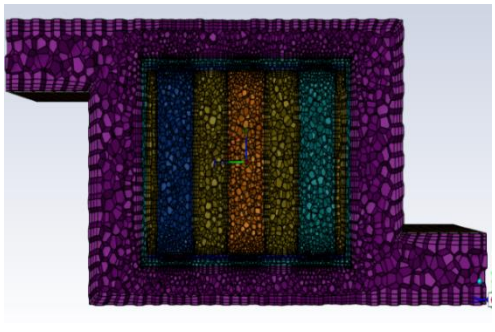

Figure 3-32: Z shaped mesh

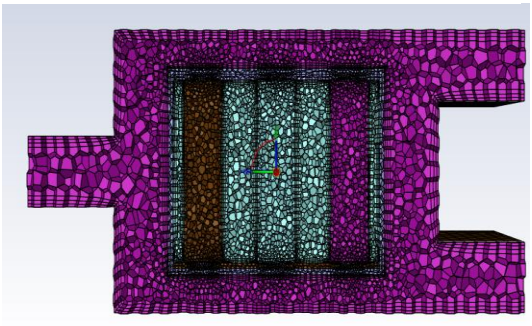

Figure 3-33: SIDO mesh

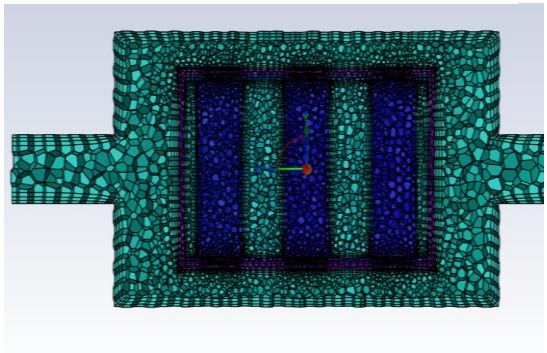

Figure 3-34: SISO mesh

CHAPTER FOUR: RESULTS AND DISCUSSION

4.1 Heat Generation

It is very important to know the value of associated heat generation of cells. To ensure the safe and proper operation of a battery, heat generation estimation is combined with thermal models in order to evaluate the temperature of the battery during use. This information is then utilized to optimize the design of the battery pack and cooling system to meet the thermal requirements of the battery (Gallo et.al).

The validated method for its measurement is done by accelerating rate calorimeter or isothermal calorimeter. However, we have found various parameters of heat generation equation and applied in it to get value of heat generation.

Assumptions

1. Heat generation for cells is measured by calorimeter for accuracy but we have used resistance method and charge-discharge technique for measurement of parameters associated with it.
2. Irreversible joule's heat is approximated from heat loss due to difference in OCV (Open Circuit Voltage) and operation potential.
3. Reversible entropic heat is approximated from the relation of the change in temperature and OCV.
4. Heat produced by self - discharge, side reaction, polarization reaction etc. are not considered for heat generation.
5. For reversible heat in discharge cycle, ambient temperature is 295K.
6. Few data points are taken for variation of temperature with change in OCV for determination of entropic coefficient.
7. Cell behavior is considered the same for charge and discharge cycle.

Experimental parameters

Internal resistance of cell

Table 4-1: Electrical parameters

S. N	Parameters	Symbol	Unit	Value
1	Open Circuit Voltage	OCV	V	3.45
2	Terminal Voltage	V	V	3.43
3	Resistor	R	Ohm	103.4
4	Current through resistor	Ir	A	0.032

The value mentioned above are of electrical parameters found for calculation of internal resistance cell. This is important for calculation of Joule's heat developed in cell.

Table 4-2: Charging-discharging of cell

S. N	Parameters	Symbol	Unit	Value
1	Temperature	T	K	295
2	Open Circuit Voltage	E	V	3.6
3	Average current drawn	I	A	2.13
4	OCV at Temperature1	OCV_1	V	3.51
5	OCV at Temperature2	OCV_2	V	3.5
6	Temperature at OCV1	T_1	K	300.2
7	Temperature at OCV2	T_2	K	301.8

The parameters above are found during charge discharge module for calculation of reversible heat in cell.

Table 4-3: Calculations of heat generation

S. N	Parameters	Symbol	Unit	Value
1	Internal resistance	r	Ohm	0.625
2	Change in temperature	dT	K	1.6
3	Change in voltage	dV	V	-0.01
4	Joule's heat	Qj	W	4.8299
5	Entropic heat	Qr	W	-3.9271
6	Total heat	Q	W	0.9028

The table above is calculation of total heat generation. Negative sign in entropic heat indicated that system is losing heat during discharge and there is decrease in randomness of system with respect to surrounding.

4.2 Unit Cell Module Cooling

4.2.1 Experimental Results

The experiment is conducted for unit-module cell cooling using air cooling at average 0.85C rate without forced convection at initial stage. Here, a charging-discharging module is used for charging and discharging cells. Then, cooling is done at a velocity of 1.3 m/s, 3.2 m/s and 4.3 m/s due to varying voltage from power source. There is variation in temperature with increase in time for charging cycle which is

equivalent to discharging cycle. Graphical analysis is done from experimental data for better understanding the trend of temperature variation with velocity.

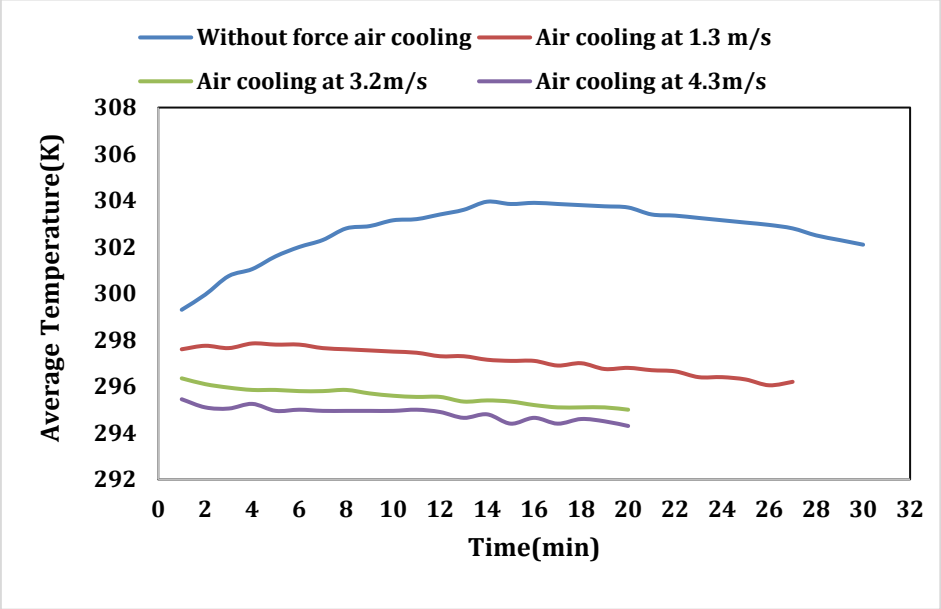

Figure 4-1: Average temperature vs time graph

Our limitation is smart charging/discharging module which decreased the amount of current as the charging time increases. The variation of current with respect to time can be observed as:

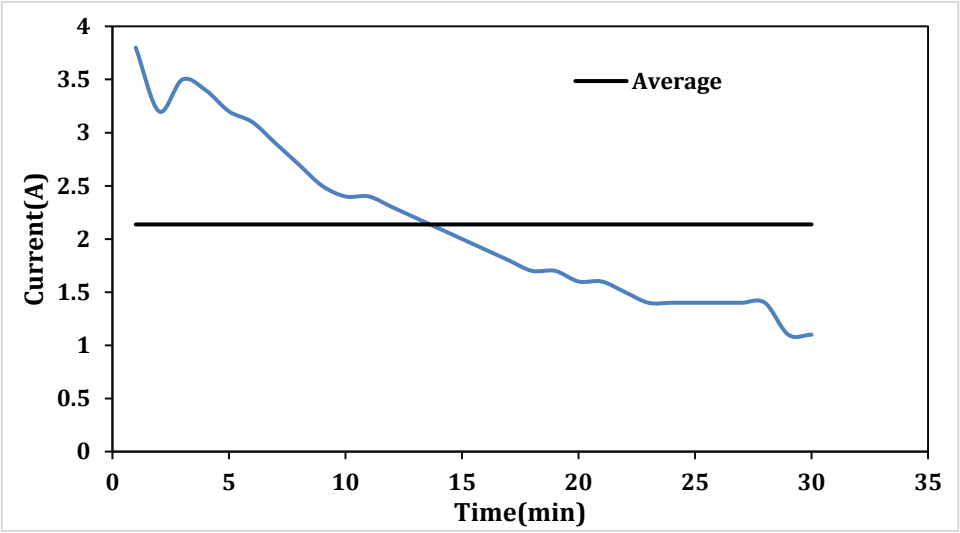

Figure 4-2: Current vs time graph

The average current is 2.13A. From the experiment at four different flow rates, following steady state mean temperature can be observed.

Table 4-4: Experimental value of temperature at different velocity

S. N	Velocity(m/s)	Experimental(K)
1	0.2	302.3
2	1.3	297.6
3	3.2	295.85
4	4.3	294.95

4.2.2 Direct Simulation Results

The values of design parameters for the analysis are provided as an input in the processing stage in Ansys fluent 2022R1.The average temperature is measured using conjugate heat transfer analysis. 0.8mm thick aluminum shell is used. The CAD model is subjected to varying air inlet velocities at 295K ambient temperature. 0.9028W is

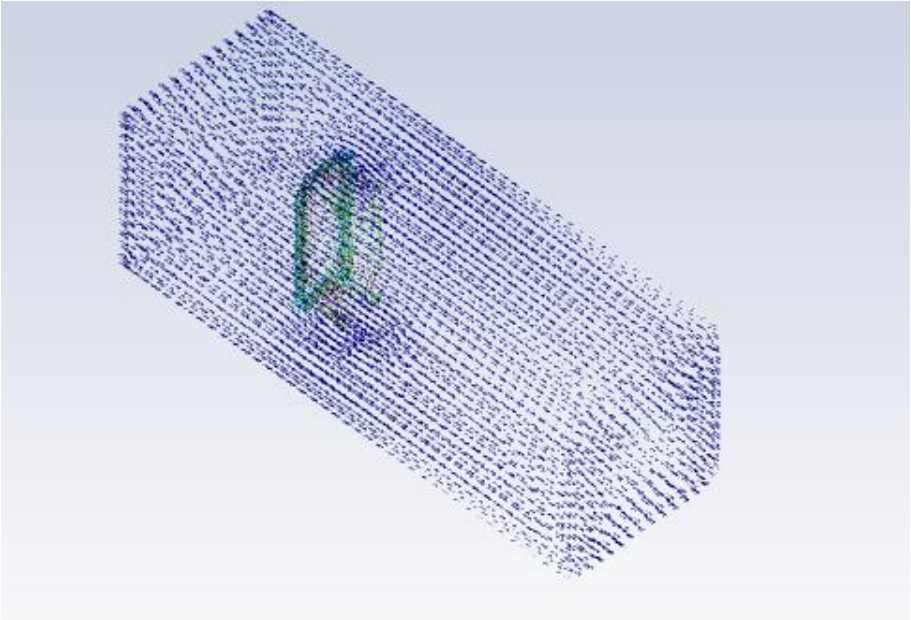

Figure 4-3: Vector of static temperature

heat generation per cell and 2.13A average current is flowing through electrode causing joule's law of heating.

Air inlet velocity is varied four times to observe the cell average temperature as shown:

Table 4-5: Simulation result of cell average temperature

S. N	Velocity(m/s)	Direct Numerical(K)
1	0.2	309.28
2	1.3	301.37
3	3.2	299.76
4	4.3	299.462

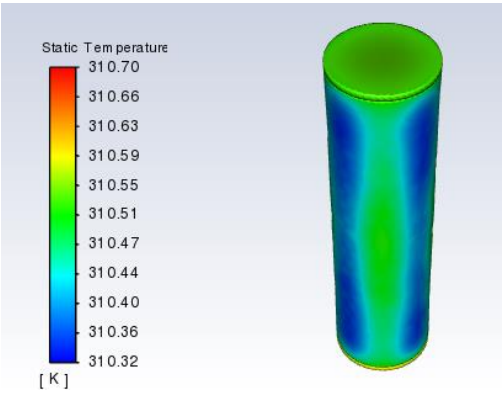

Figure 4-4:Temperature distribution at 0.2m/s

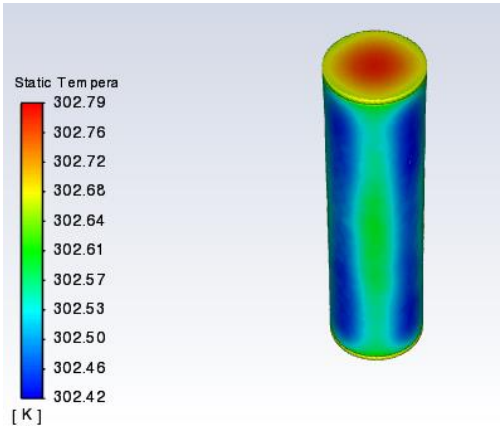

Figure 4-5:Temperature distribution at 1.3m/s

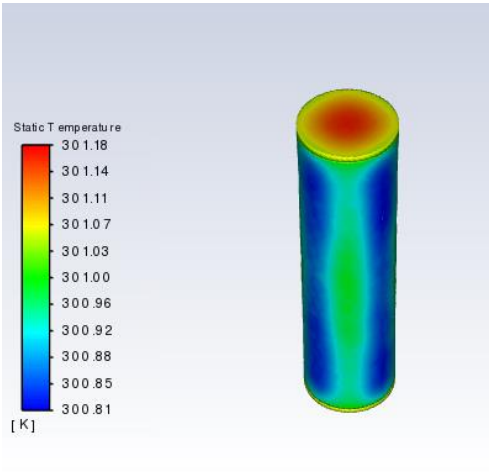

Figure 4-6:Temperature distribution at 3.2m/s

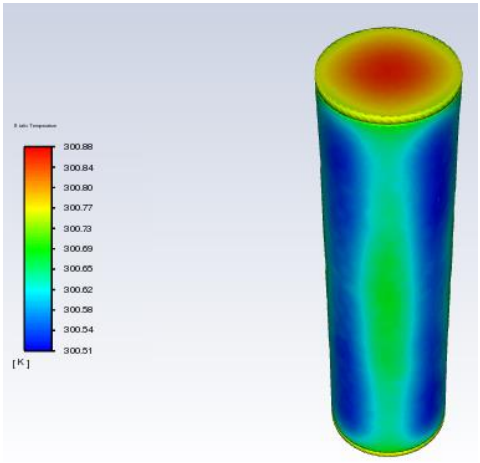

Figure 4-7:Temperature distribution at 4.3m/s

From the analysis, we can observe that the cell average temperature at four different velocities that lower velocities creates higher temperature and higher velocities creates lower cell average temperature. Temperature distribution within a cell can be analyzed through counter plots. The temperature gradient at the busbar seems quite sharp at high flow rates than lower flow rate.

4.2.3 Response Surface Results

The design parameters which can affect the "Average Cell Temperature" of the system are aluminum thickness, air inlet velocity and ambient temperature. Varying inputs and output are defined in the design of experiments. Air inlet velocity varies from 0.1 to 5m/s constrained by fan capacity as an input. Sparse Grid initialization is used to define the design of experiments to observe cell average temperature as an output.

Table 4-6:Design of experiments

S. N	Velocity(m/s)	Temperature(K)
1	0.1	312.96
2	2.55	300.06
3	5	299.33

Using the above data as an experiment, response surface is fitted using sparse grid with number of refinement points.

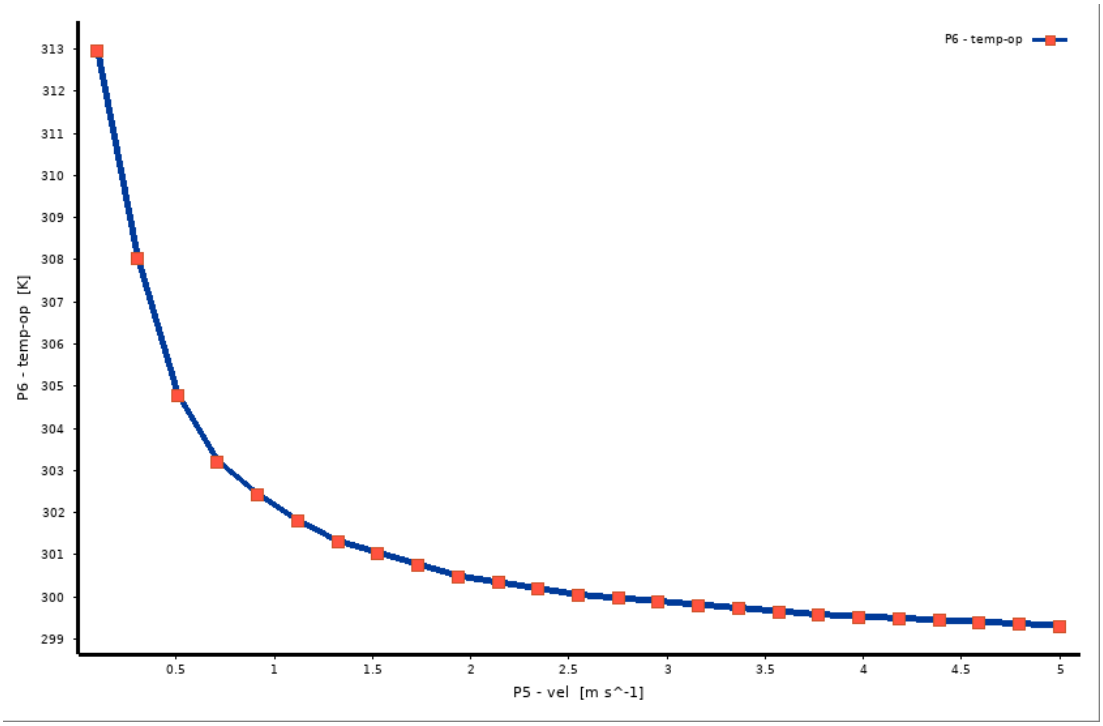

Figure 4-8: Response curve of temperature vs velocity

Of the available points generated through, optimization is done for seeking temperature at given velocity using screening method. The following result is obtained.

Table 4-7: Response surface results

S. N	Velocity(m/s)	Response Surface(K)
1	0.2	310.545
2	1.3	301.39
3	3.2	299.81
4	4.3	299.47

4.2.4 Discussion

It is found that cell average temperature decreased with increase in air velocity from both direct numerical analysis and response surface analysis. This is because of the increment in the convective heat rate. From experimental analysis of unit cell module, it is found that there is decrease in cell average temperature with increase in velocity.

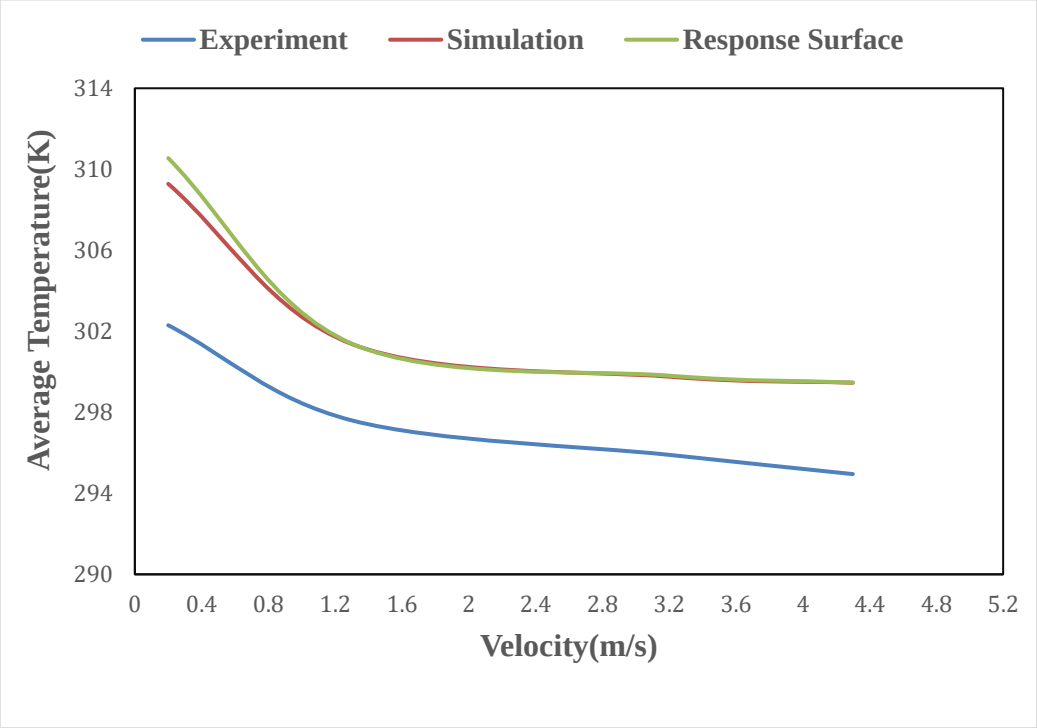

Figure 4-9: Comparison of average temperature. vs velocity

There is a decrease in temperature from 302.3K to 294.95^{0}C from 0.2 m/s to 4.3m/s which showed positive effect of force air convection on cooling of cell. There is a net average deviation of 1.6% on simulation and 1.71% on response surface result from experimental value.

Simulation may not capture the behavior of real system due to modeling simplifications. Various other forms of heat exchange might occur in experiments not modeled for numerical analysis. The result deviation occurs due to simplified assumption of model on electric and thermal material properties. There is also role of environmental condition such as temperature, humidity etc. which are encountered in performing experiment are not accounted in simulation.

Table 4-8:Comparison of experimental value vs response surface value

S. N	Velocity(m/s)	Experimental (K)	Direct Simulation (K)	Response Surface (K)	Error Direct Numerical	Error Response Surface
1	0.2	302.3	309.28	310.55	2.31%	2.73%
2	1.3	297.6	301.37	301.39	1.27%	1.27%
3	3.2	295.85	299.76	299.81	1.32%	1.34%
4	4.3	294.95	299.46	299.47	1.53%	1.53%

A cell's average temperature is calculated based on 2 points on the cell and steady state value is taken as our final cell average temperature value. This shows that deviation might occur due to error in accuracy of measurement. Our simulation is performed at constant C rate of 0.85C which is value of average C rate on experiment during charging/discharging cycle. So, the facts above clarify the reason behind deviation between experiment and simulated results.

4.3 Cold Pate Cooling

4.3.1 Parametric Analysis

Four cold plate configurations are taken for analysis with varying velocities from 0.4m/s to 5m/s. First, cells' average temperature is analyzed with respect to velocities in the given range using CHT analysis. Response surface is drawn based on limited number of experiments using sparse grid analysis. The variation of cell average temperature can be observed in the graph.

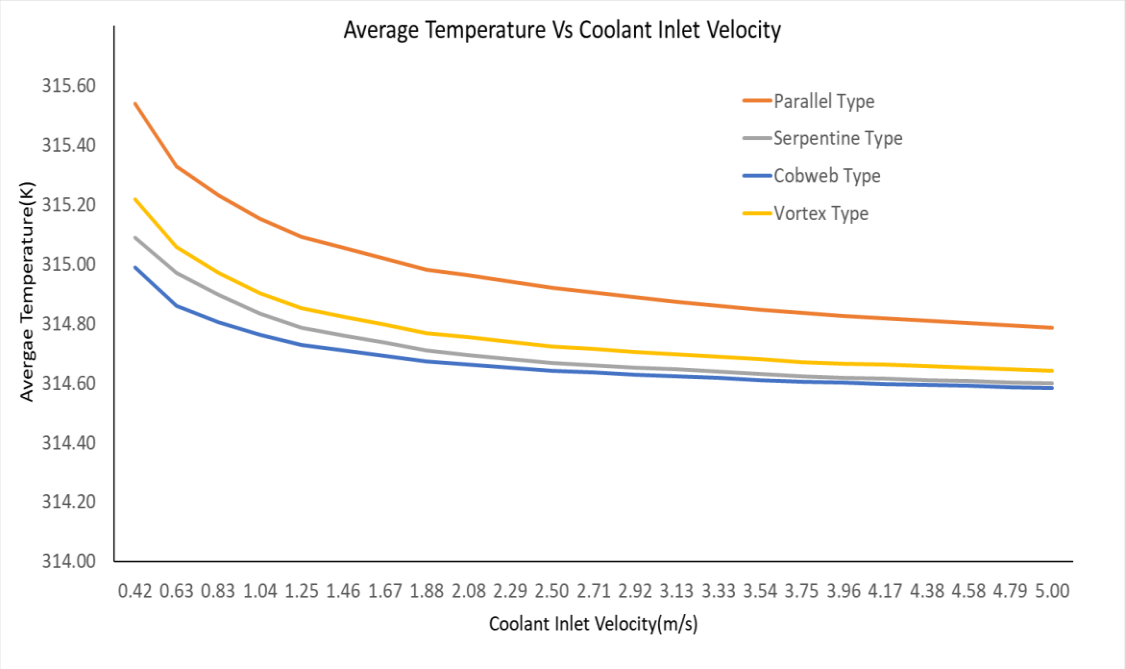

Figure 4-10: Graph of average temperature vs velocity

It is clear from the above graph average cell temperature of cobweb type is least for the same coolant inlet velocity. The nature of the average cell temperature decreases until a certain inlet velocity. After that increase in velocity will have lesser impact on cell average temperature.

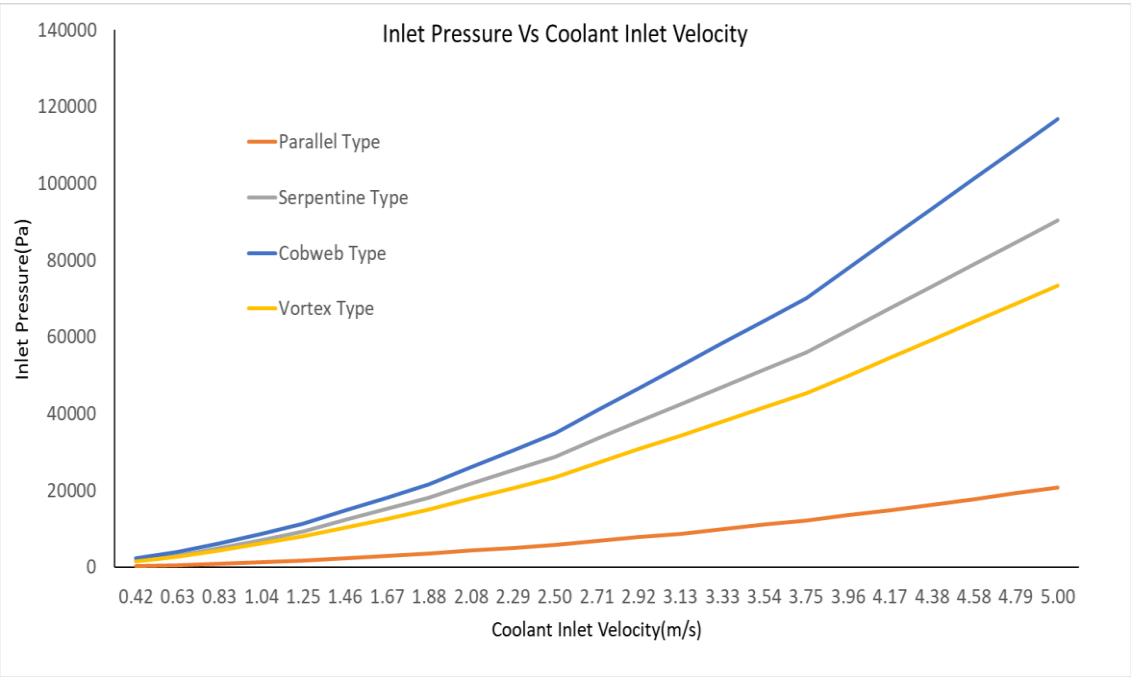

Figure 4-11: Inlet pressure vs coolant inlet velocity

Inlet pressure must vary parabolically, but the above graph predicts the variation to be linear with increasing velocity. Inlet pressure directly signifies the pumping power required to flow the coolant through flow channel. The inlet pressure for parallel type flow channel seems to be less than vortex type which is less than serpentine type cooling configuration. Cobweb type cooling type has the highest inlet pressure at the same velocity.

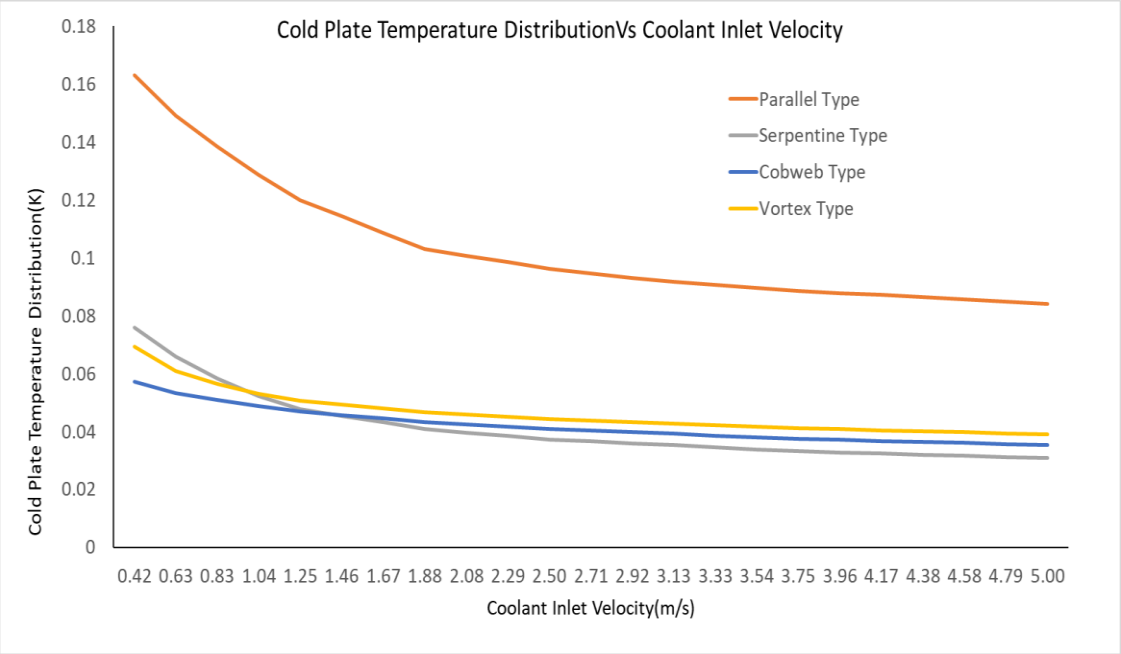

Figure 4-12: Cold plate temperature distribution vs coolant inlet velocity

The distribution of temperature is also observed numerically using standard deviation of static temperature at the face of cold plate which is interface of thermal exchange between module and coolant path. The Cobweb type cold plate has more uniform temperature distribution until about 1.5m/s. Above that pressure serpentine type has the most uniform temperature distribution.

4.3.2 CHT Simulation

Fristly,module analysis without any cold plate is done to observe the heat generation and temperature distribution inside the module.The volume average temperature at 0.05m/s air velocities is 334.62K with static temperature distribution as:

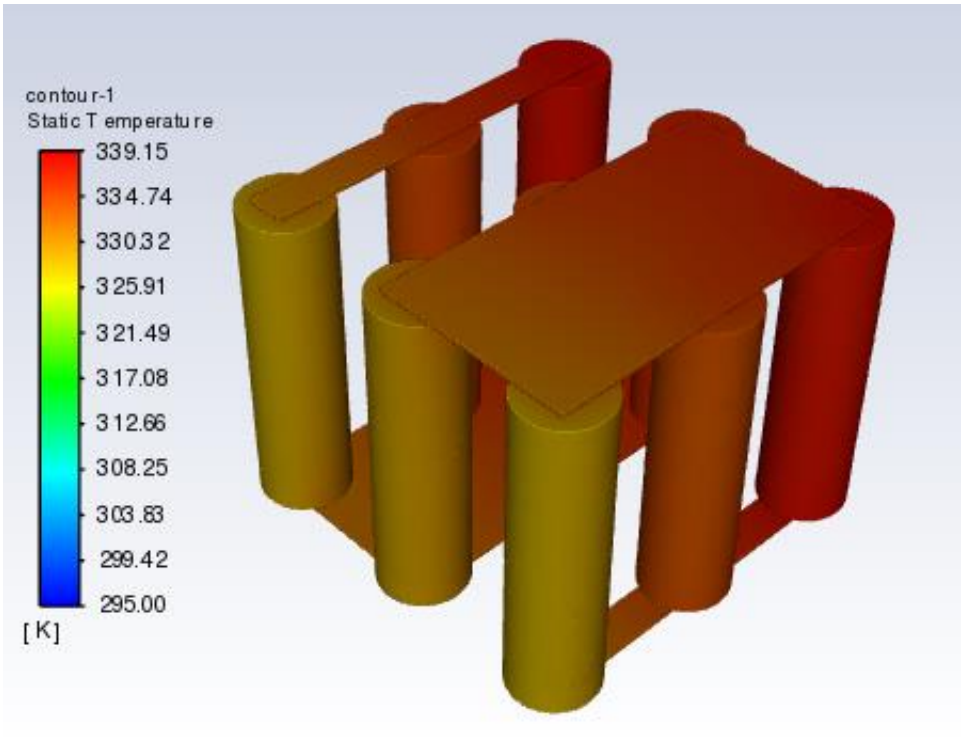

Figure 4-13: Module temperature contour plot

From the parametric analysis, the average cell temperature variation with coolant inlet velocities can be observed. The minimum coolant inlet velocities where the temperature tends to stabilize for every configuration is around 1m/s subjected to the boundary condition.

From the above plots and the data acquired, we can observe that parallel type cold plate performs worse than other type cooling plates. Compared to parallel type cooling plate at given condition, vortex type is 0.07% better for minimizing the cell average temperature, serpentine type is 0.102% better than parallel type. The temperature distribution of each type of cold plate can be observed through a contour plot below at same coolant inlet velocity 1m/s with inputs such as heat generation rate 0.9028W, tab currents 2.13A at ambient temperature 295K.

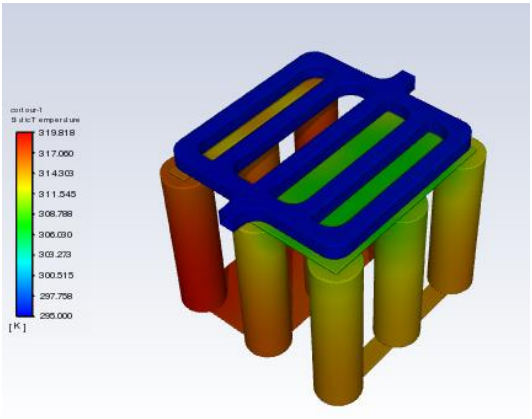

Figure 4-14: Temperature contour parallel type

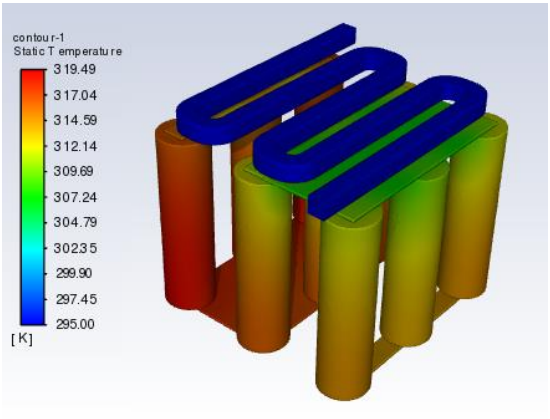

Figure 4-15: Temperature contour serpentine type

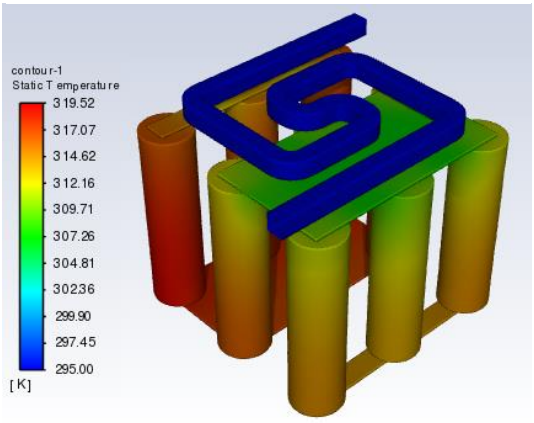

Figure 4-16: Temperature contour vortex type

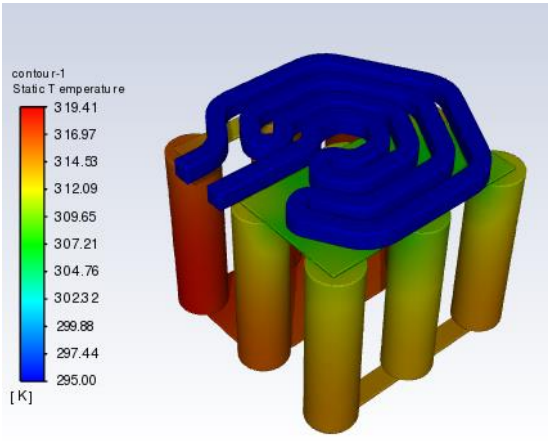

Figure 4-17: Temperature contour cobweb type

Cobwebs are best compared to other types of cooling plates. It is 0.124% better at lowering the temperature relative to parallel type cooling plate while geometric and inlet conditions are fixed.Also, Cold plate for good interfacial temperature distribution is Cobweb type followed by serpentine followed by vortex type. The performance of parallel type cold plate for interfacial temperature distribution is the worst.

4.4 Module Air Cooling

4.4.1 Parametric Analysis

Different configurations of the flow channel are designed and analyzed for the air-cooling system such as U shaped, Z shaped, SISO, SIDO. Velocity ranging from 0.1m/s to 40 m/s were supplied to cool the battery pack. Then, the cell average temperature is analyzed for the varying velocities using CHT analysis. Response surface is drawn based on limited no. of experiments using Sparse grid analysis. The variation of cell average temperature with air velocity is observed as:

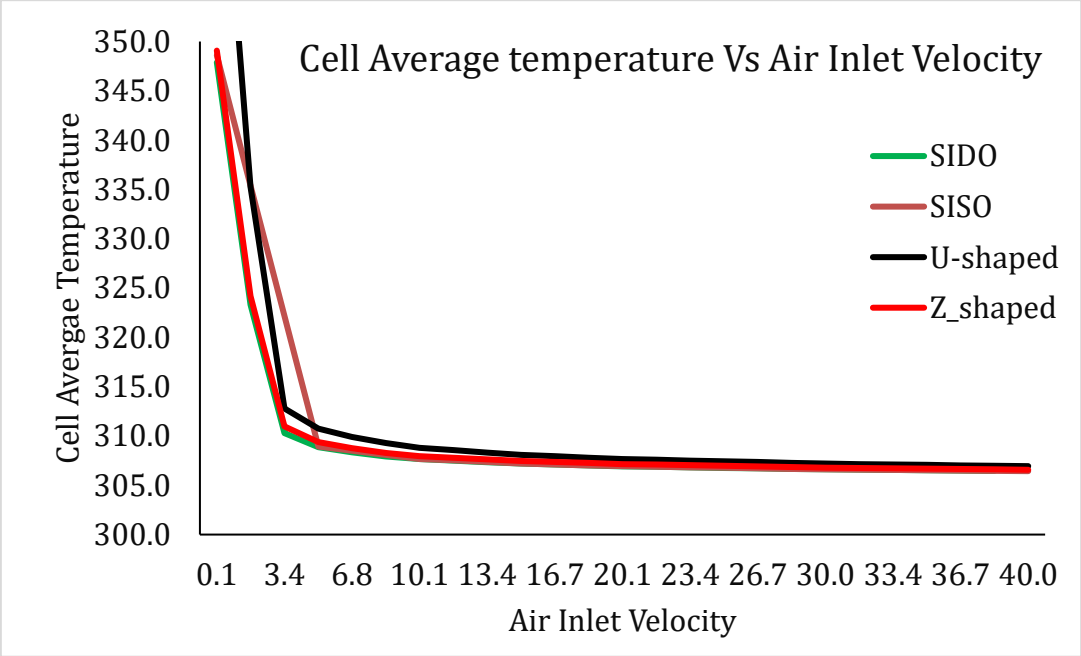

Figure 4-18: Average temperature vs velocity for different geometries

As the velocity of supply cooling air is increasing, the graph explains that the cell average temperature of all types of the configuration is decreasing from velocity of 0.1m/s to 40m/s. This is result of surface response comparison from sparse grid which give value based on approximate function. On that basis it is seen that SIDO shaped has low cell average temperature

4.4.2 CHT Simulation

Above certain velocity, design configuration does not have significant impact on cell average temperature.

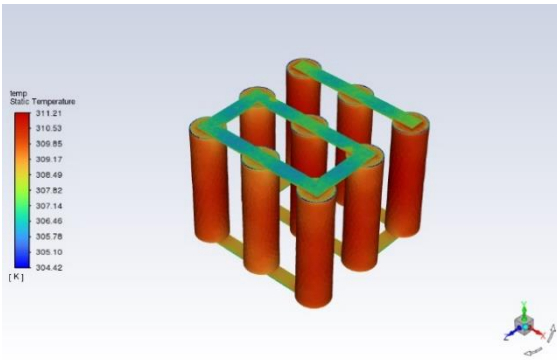

Figure 4-19:Temperature contour Z shaped

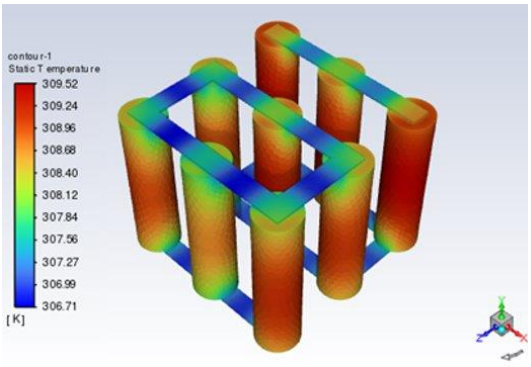

Figure 4-20:Temperature contour U shaped

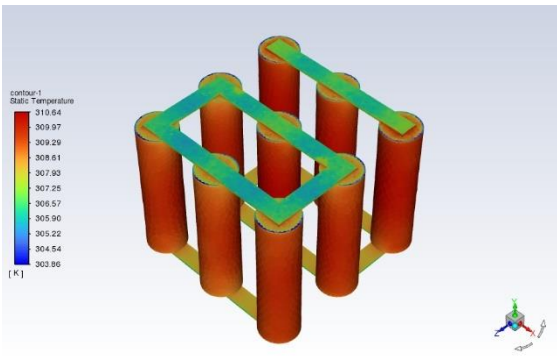

Figure 4-21:Temperature contour SISO

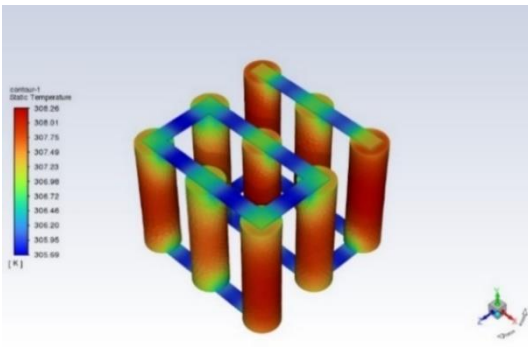

Figure 4-22:Temperature contour SIDO

The air inlet velocity of 10 m/s is supplied for all types of configurations and corresponding temperature contour is obtained. The temperature contour shows that the average cell temperature of SIDO configuration is low as compared to the other configurations. The corresponding cell average temperature for SISO, SIDO, U-shape, and Z-shape are 307.68K,307.60K,308.81K and 308.02K, respectively. Among these configurations, the average cell temperature of SIDO is less than other. From direct simulation, SIDO configuration is effective for air cooling of 3S3P module. It shows that there is difference in value obtained from surface response and direct simulation. This describes the insufficiency of response surface to approximate the temperature at given points.

4.5 Cost Estimation and Analysis

Cost estimation accuracy is critical for efficient project administration and decision-making. Our project comprises the cost of material required for experimental setup which is the cost price of the material in market. It has included tentative travelling cost for working on experimental setup, project place etc. Computational cost is linked with involvement in the total working period of project in both extensive study and implementation of study.

Table 4-9: Cost estimation

S. N	Description	Cost (Rs)
1	Cell	980
2	Thermocouple system	1600
3	Fan	1000
4	Polyamide Tape	230
5	Arduino	1600
6	Wires	150
7	Thermocouple	600
8	Test Cell	100
9	Plywood	600
10	Aluminum container	400
11	Computational cost	30000
12	Utility cost	6000
13	Travelling expenses	2000
14	Total cost	45260

CHAPTER FIVE: CONCLUSION AND RECOMMENDATIONS

5.1 Conclusion

In this project we have calculated heat generation of INR-18650-25s lithium-ion cell. Then unit cell module cooling system is designed and simulated. The analysis system is validated and verified by comparing simulated and parametric temperature values with experimental values and good agreement is achieved. Similarly, lithium-ion battery 3S3P module is designed for both air cooling under four different configurations and simulated. It is also done for liquid cold plate cooling system under 4 different configurations. This is done to find an appropriate cooling system. The conclusion that can be drawn from this project are:

1. Heat generation of lithium-ion INR-18650-25s is found to be 0.9028W at 0.85C rate.
2. There is a decrease in temperature from 302.3K to 294.95^{0}C from 0.2 m/s to 4.3m/s due to an increase in force air convection on cooling of unit cell module. There is a net average deviation of 1.6% on direct simulation and 1.71% on response surface result from experimental value on unit cell module air cooling system.
3. Four different cold plate configurations parallel path, vortex type, serpentine type and cobweb are taken for analysis with varying velocities from 0.4m/s to 5m/s. Among them, cobweb is found to have less cell average temperature for that range of flow velocity. Average cell temperature of cobweb type is least for all range of the coolant inlet velocity from simulation. The cobweb type cold plate has a more uniform temperature distribution of about 1.5m/s. Above that pressure, serpentine type has the most uniform temperature distribution.
4. Four different configurations such as U shaped, Z shaped, SISO, SIDO of the flow channel are designed and analyzed for the flow velocity ranging from 0.1 m/s to 40 m/s. It is found that SIDO shaped channel has low average temperature compared to other configurations from surface response analysis and simulation result.

5.2 Recommendations

This project is only limited to three different flow velocity for experiment of unit cell module cooling system This project is only limited to 3S3P module of cooling system. The comparative analysis of module air cooling system is done only based on cell average temperature with variation in inlet flow channel. For liquid cold plate cooling it is only limited to cell average temperature and pressure difference with respect to variation in coolant flow velocity for four different configurations of same inlet cross section. So, the works that can be done in future for further exploration are given below:

1. Acceleration rate calorimeter can provide accurate heat generation rate with proper charge discharge rate.
2. Unit cell module cooling with varied number of cooling velocity can be done experimentally to know stable range of velocity for developing optimized cooling module.
3. Parametric analysis of 3S3P module cooling can be extended by increasing the number of parameters which affects the module performance.
4. Experimental validation of 3S3P module air cooling and cold plate liquid cooling can be done to find optimize system economically.

REFERENCES

Amorim, A. S. C. M. de, Pessoa, F. L. P., & Calixto, E. E. da S. (2022). *Battery Thermal Management System for Electric Vehicles: a Brief Review*. 9–15. https://doi.org/10.5151/siintec2021-205611

Behi, H., Karimi, D., Behi, M., Ghanbarpour, M., Jaguemont, J., Sokkeh, M. A., Gandoman, F. H., Berecibar, M., & Van Mierlo, J. (2020). A new concept of thermal management system in Li-ion battery using air cooling and heat pipe for electric vehicles. *Applied Thermal Engineering*, *174*(November 2019), 115280. https://doi.org/10.1016/j.applthermaleng.2020.115280

Chen, D., Jiang, J., Kim, G. H., Yang, C., & Pesaran, A. (2016). Comparison of different cooling methods for lithium ion battery cells. *Applied Thermal Engineering*, *94*, 846–854. https://doi.org/10.1016/j.applthermaleng.2015.10.015

Chen, K. H., Han, T., Khalighi, B., & Klaus, P. (2017). Air cooling concepts for Li-ion battery pack in cell level. *ASME 2017 Heat Transfer Summer Conference, HT 2017*, *1*(July). https://doi.org/10.1115/HT2017-4701

Chen, Y., & Evans, J. W. (1996). *Thermal Analysis of Lithium-Ion Batteries*. *143*(9), 2708–2712.

Choudhari, V. G., Dhoble, D. A. S., & Sathe, T. M. (2020). A review on effect of heat generation and various thermal management systems for lithium ion battery used for electric vehicle. *Journal of Energy Storage*, *32*(August), 101729. https://doi.org/10.1016/j.est.2020.101729

Deng, T., Zhang, G., Ran, Y., & Liu, P. (2019). Thermal performance of lithium ion battery pack by using cold plate. *Applied Thermal Engineering*, *160*(66), 114088. https://doi.org/10.1016/j.applthermaleng.2019.114088

Dubey, P., Pulugundla, G., & Srouji, A. K. (2021). Direct comparison of immersion and cold-plate based cooling for automotive li-ion battery modules. *Energies*, *14*(5). https://doi.org/10.3390/en14051259

Fotouhi, A., Auger, D. J., Propp, K., Longo, S., & Wild, M. (2016). A review on electric vehicle battery modelling: From Lithium-ion toward Lithium-Sulphur. *Renewable and Sustainable Energy Reviews*, *56*, 1008–1021. https://doi.org/10.1016/j.rser.2015.12.009

Gregory L. Plett. (2015). *Battery Modeling*.

Hui Zhang, E. A. (2013). AIR MOVEMENT PREFERENCES OBSERVED IN OFFICE BUILDINGS. *International Journal of Biometeorology*, *15*(4), 250–260. https://doi.org/https://escholarship.org/uc/item/4gp5385f

Huo, Y., Rao, Z., Liu, X., & Zhao, J. (2015). Investigation of power battery thermal management by using mini-channel cold plate. *Energy Conversion and Management*, *89*, 387–395. https://doi.org/10.1016/J.ENCONMAN.2014.10.015

Jarrett, A., & Kim, I. Y. (2011). Design optimization of electric vehicle battery cooling plates for thermal performance. *Journal of Power Sources*, *196*(23), 10359–10368. https://doi.org/10.1016/j.jpowsour.2011.06.090

Jeon, D. H. (2014). Numerical modeling of lithium ion battery for predicting thermal behavior in a cylindrical cell. *Current Applied Physics*, *14*(2), 196–205. https://doi.org/10.1016/j.cap.2013.11.006

Jiaqiang, E., Xu, S., Deng, Y., Zhu, H., Zuo, W., Wang, H., Chen, J., Peng, Q., & Zhang, Z. (2018). Investigation on thermal performance and pressure loss of the fluid cold-plate used in thermal management system of the battery pack. *Applied Thermal Engineering*, *145*(July), 552–568. https://doi.org/10.1016/j.applthermaleng.2018.09.048

Kim, J., Oh, J., & Lee, H. (2019). Review on battery thermal management system for electric vehicles. *Applied Thermal Engineering*, *149*(November 2018), 192–212. https://doi.org/10.1016/j.applthermaleng.2018.12.020

Kizilel, R., Sabbah, R., Selman, J. R., & Al-Hallaj, S. (2009). An alternative cooling system to enhance the safety of Li-ion battery packs. *Journal of Power Sources*,

194(2), 1105–1112. https://doi.org/10.1016/j.jpowsour.2009.06.074

Lai, Y., Du, S., Ai, L., Ai, L., & Cheng, Y. (2015). ScienceDirect Insight into heat generation of lithium ion batteries based on the electrochemical-thermal model at high discharge rates. *International Journal of Hydrogen Energy*, *40*(38), 13039–13049. https://doi.org/10.1016/j.ijhydene.2015.07.079

Liu, C., Xu, D., Weng, J., Zhou, S., Li, W., Wan, Y., Jiang, S., Zhou, D., Wang, J., & Huang, Q. (2020). Phase change materials application in battery thermal management system: A review. *Materials*, *13*(20), 1–37. https://doi.org/10.3390/ma13204622

Liu, K., Li, K., Peng, Q., & Zhang, C. (2019). A brief review on key technologies in the battery management system of electric vehicles. *Frontiers of Mechanical Engineering*, *14*(1), 47–64. https://doi.org/10.1007/s11465-018-0516-8

Liu, S., Liu, X., Dou, R., Zhou, W., Wen, Z., & Liu, L. (2020). Experimental and simulation study on thermal characteristics of 18,650 lithium–iron–phosphate battery with and without spot–welding tabs. *Applied Thermal Engineering*, *166*, 114648. https://doi.org/10.1016/j.applthermaleng.2019.114648

Lu, Z., Yu, X. L., Wei, L. C., Cao, F., Zhang, L. Y., Meng, X. Z., & Jin, L. W. (2019). A comprehensive experimental study on temperature-dependent performance of lithium-ion battery. *Applied Thermal Engineering*, *158*(December 2018). https://doi.org/10.1016/j.applthermaleng.2019.113800

Lu, Z., Yu, X., Wei, L., Qiu, Y., Zhang, L., Meng, X., & Jin, L. (2018). Parametric study of forced air cooling strategy for lithium-ion battery pack with staggered arrangement. *Applied Thermal Engineering*, *136*, 28–40. https://doi.org/10.1016/j.applthermaleng.2018.02.080

Manikandan, B., Yap, C., & Balaya, P. (2017). Towards Understanding Heat Generation Characteristics of Li-Ion Batteries by Calorimetry, Impedance, and Potentiometry Studies. *Journal of The Electrochemical Society*, *164*(12), A2794–A2800. https://doi.org/10.1149/2.1811712jes

Manzetti, S., & Mariasiu, F. (2015). Electric vehicle battery technologies : From present state to future systems. *Renewable and Sustainable Energy Reviews*, *51*, 1004–1012. https://doi.org/10.1016/j.rser.2015.07.010

Mokashi, I., Khan, S. A., Abdullah, N. A., Bin Azami, M. H., & Afzal, A. (2020). Maximum temperature analysis in a Li-ion battery pack cooled by different fluids. *Journal of Thermal Analysis and Calorimetry*, *141*(6), 2555–2571. https://doi.org/10.1007/s10973-020-10063-9

Panchal, S., Mathew, M., Fraser, R., & Fowler, M. (2018). Electrochemical thermal modeling and experimental measurements of 18650 cylindrical lithium-ion battery during discharge cycle for an EV. *Applied Thermal Engineering*, *135*(October 2017), 123–132. https://doi.org/10.1016/j.applthermaleng.2018.02.046

Peng, X., Cui, X., Liao, X., & Garg, A. (2020). A thermal investigation and optimization of an air-cooled lithium-ion battery pack. *Energies*, *13*(11). https://doi.org/10.3390/en13112956

Pesaran, A. A., Burch, S., & Keyser, M. (1999). An Approach for Designing Thermal Management Systems for Electric and Hybrid Vehicle Battery Packs Preprint. *The Fourth Vehicle Thermal Management Systems Conference and Exhibition 24-27*, *January*, 1–18.

Rao, Z., Qian, Z., Kuang, Y., & Li, Y. (2017). Thermal performance of liquid cooling based thermal management system for cylindrical lithium-ion battery module with variable contact surface. *Applied Thermal Engineering*, *123*, 1514–1522. https://doi.org/10.1016/j.applthermaleng.2017.06.059

Roe, C., Feng, X., White, G., Li, R., Wang, H., Rui, X., Li, C., Zhang, F., Null, V., Parkes, M., Patel, Y., Wang, Y., Wang, H., Ouyang, M., Offer, G., & Wu, B. (2022). Immersion cooling for lithium-ion batteries – A review. *Journal of Power Sources*, *525*(August 2021). https://doi.org/10.1016/j.jpowsour.2022.231094

Samimi, F., Babapoor, A., Azizi, M., & Karimi, G. (2016). Thermal management analysis of a Li-ion battery cell using phase change material loaded with carbon

fibers. *Energy*, *96*, 355–371. https://doi.org/10.1016/j.energy.2015.12.064

Shang, Z., Qi, H., Liu, X., Ouyang, C., & Wang, Y. (2019). Structural optimization of lithium-ion battery for improving thermal performance based on a liquid cooling system. *International Journal of Heat and Mass Transfer*, *130*, 33–41. https://doi.org/10.1016/j.ijheatmasstransfer.2018.10.074

Tete, P. R., Gupta, M. M., & Joshi, S. S. (2021). Developments in battery thermal management systems for electric vehicles: A technical review. *Journal of Energy Storage*, *35*(January), 102255. https://doi.org/10.1016/j.est.2021.102255

Wang, X., Liu, S., Zhang, Y., Lv, S., Ni, H., Deng, Y., & Yuan, Y. (2022). A Review of the Power Battery Thermal Management System with Different Cooling, Heating and Coupling System. *Energies*, *15*(6). https://doi.org/10.3390/en15061963

Wu, H., Zhang, X., Cao, R., & Yang, C. (2021). An investigation on electrical and thermal characteristics of cylindrical lithium-ion batteries at low temperatures. *Energy*, *225*, 120223. https://doi.org/10.1016/j.energy.2021.120223

Xie, J., Ge, Z., Zang, M., & Wang, S. (2017). Structural optimization of lithium-ion battery pack with forced air cooling system. *Applied Thermal Engineering*, *126*, 583–593. https://doi.org/10.1016/j.applthermaleng.2017.07.143

Yang, N., Zhang, X., Li, G., & Hua, D. (2015). Assessment of the forced air-cooling performance for cylindrical lithium-ion battery packs: A comparative analysis between aligned and staggered cell arrangements. *Applied Thermal Engineering*, *80*, 55–65. https://doi.org/10.1016/j.applthermaleng.2015.01.049

Yang, Z., Patil, D., & Fahimi, B. (2019). Electrothermal modeling of lithium-ion batteries for electric vehicles. *IEEE Transactions on Vehicular Technology*, *68*(1), 170–179. https://doi.org/10.1109/TVT.2018.2880138

Zhang, L., Peng, H., Ning, Z., Mu, Z., & Sun, C. (2017). Comparative research on RC equivalent circuit models for lithium-ion batteries of electric vehicles. *Applied*

Sciences (Switzerland), *7*(10). https://doi.org/10.3390/app7101002

Zhao, Q., Wu, H., Wang, Z., Fan, Y., & Cheng, W. (2022). Numerical research on lithium-ion battery thermal management utilizing a novel cobweb-like channel cooling plate exchanger. *Frontiers in Energy Research*, *10*(September), 1–11. https://doi.org/10.3389/fenrg.2022.992779

Zhao, Y., Zou, B., Li, C., & Ding, Y. (2019). Active cooling based battery thermal management using composite phase change materials. *Energy Procedia*, *158*, 4933–4940. https://doi.org/10.1016/j.egypro.2019.01.697

Zhou, Y., Wang, Z., Xie, Z., & Wang, Y. (2022). *Parametric Investigation on the Performance of a Battery Thermal Management System with Immersion Cooling*. 1–21.

APPENDIX A: Additional Geometry

All dimensions are in mm

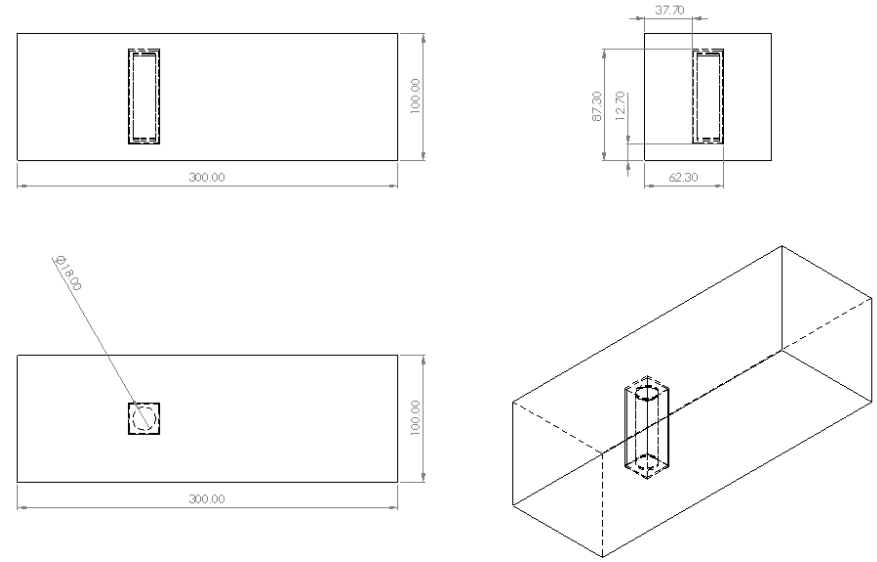

Figure A-1: Experimental setup CAD model

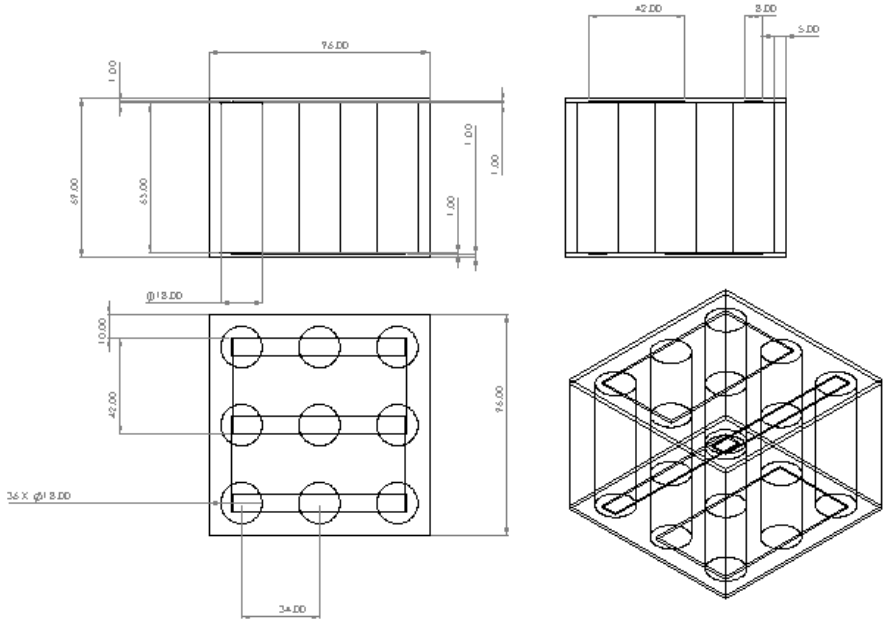

Figure A-2: Cold plate module detailed

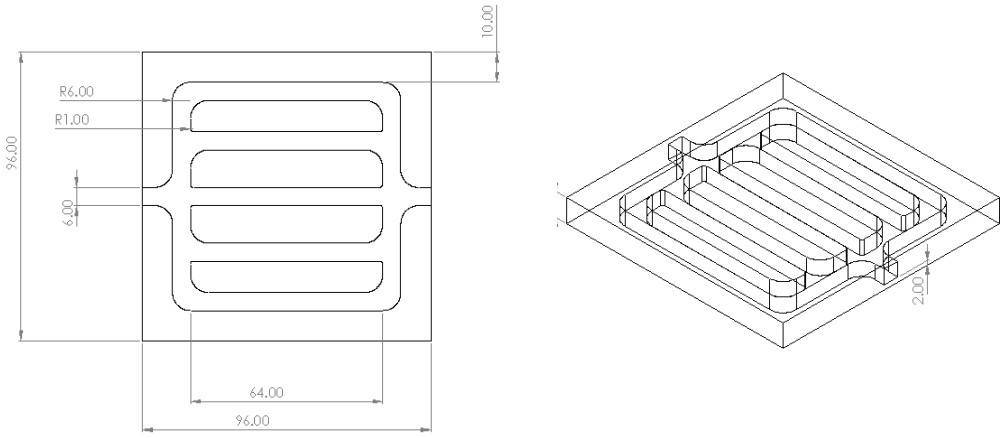

Figure A-3: Parallel type cold plate detailed

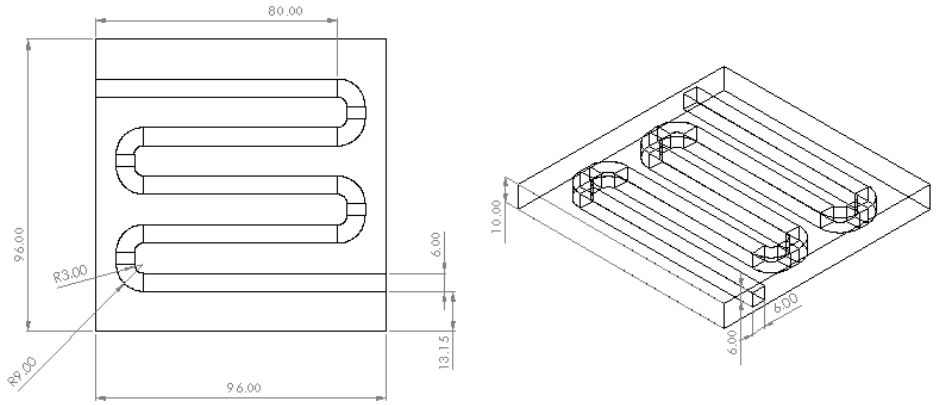

Figure A-4: Serpentine type cold plate detailed

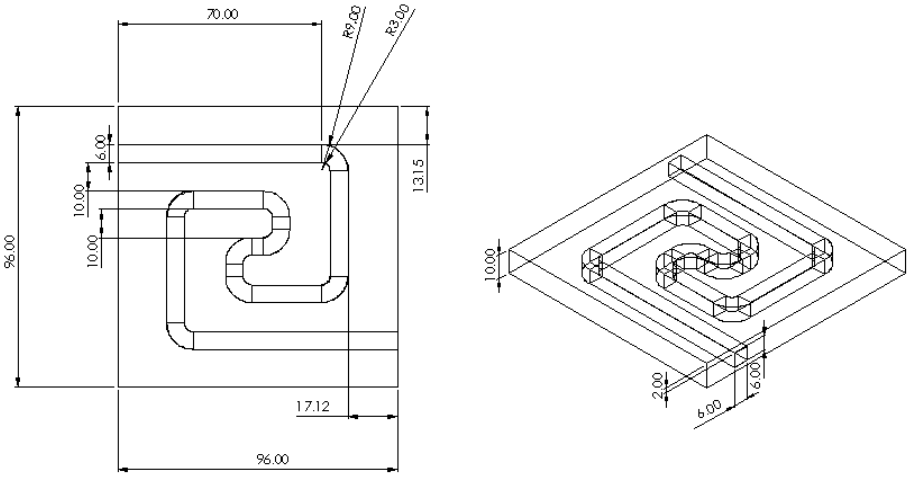

Figure A-5: Vortex type cold plate detailed

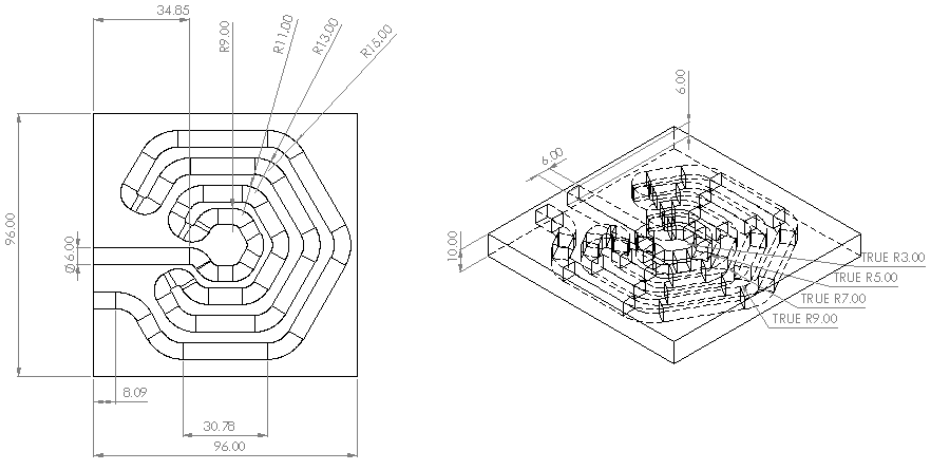

Figure A-6: Cobweb type cold plate detailed

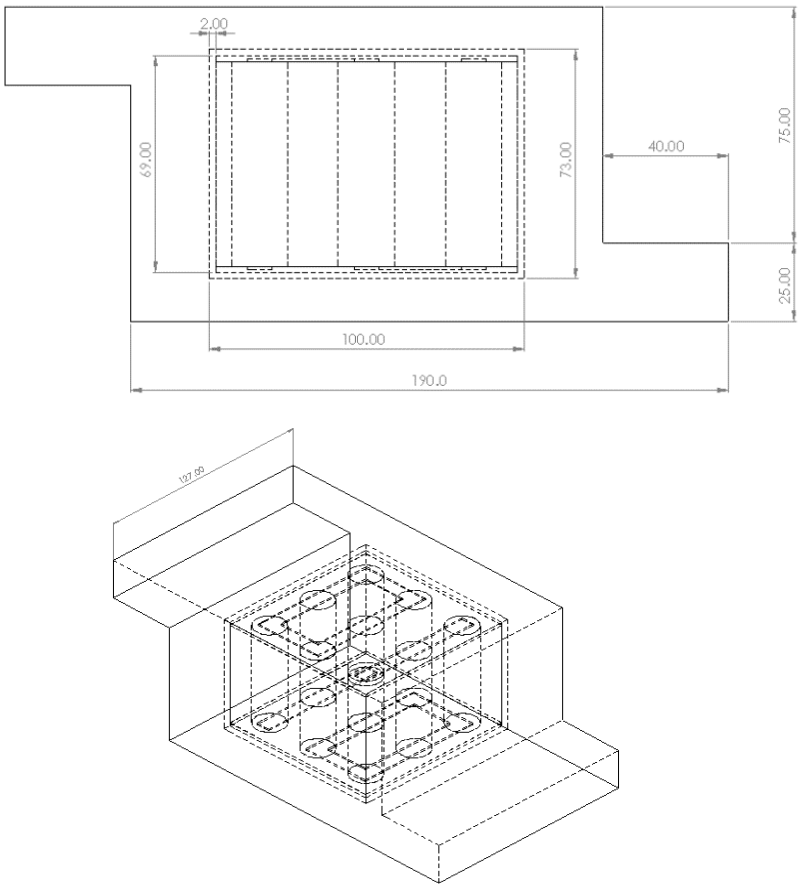

Figure A-7: Z -Shaped configuration detailed

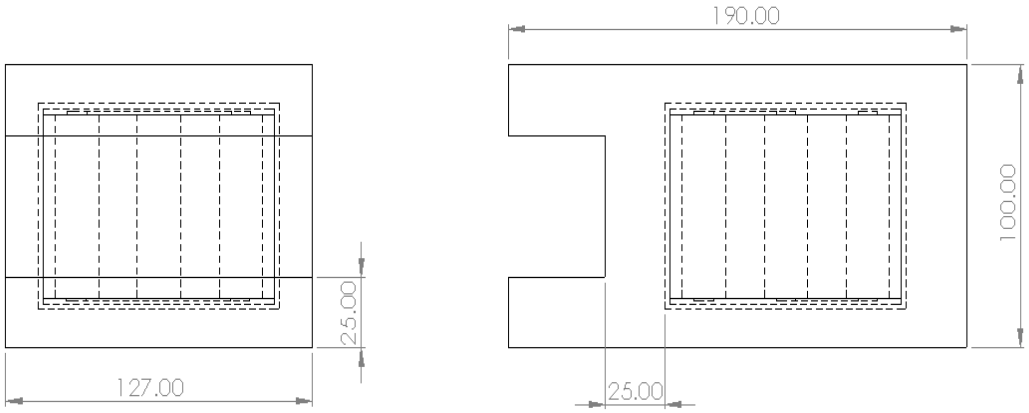

Figure A-8: U Shaped configuration detailed

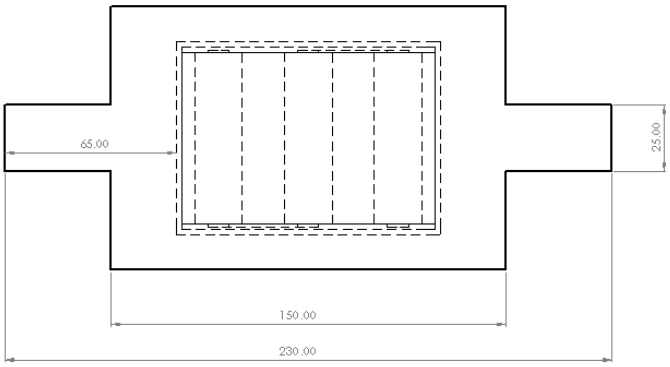

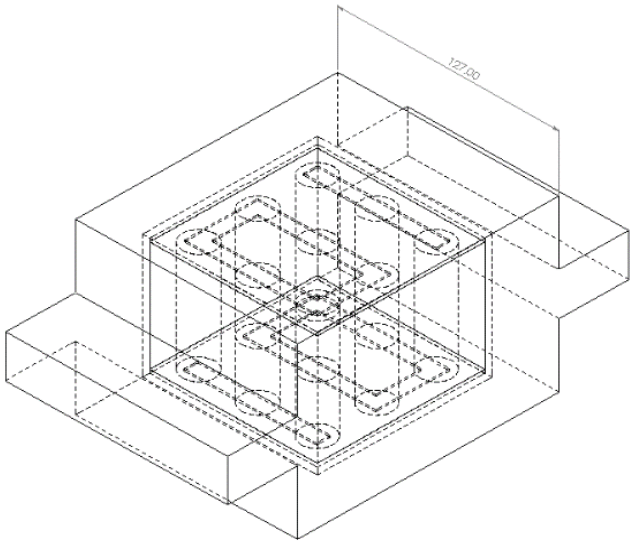

Figure A-9: SISO configuration detailed

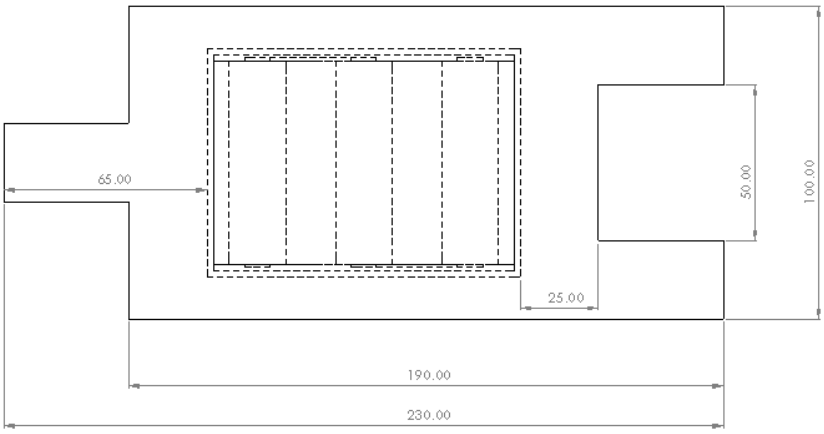

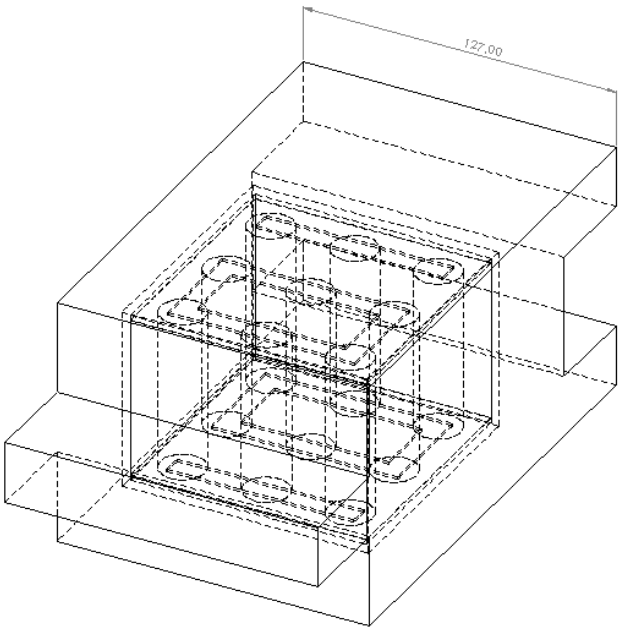

Figure A-10: SIDO configuration detailed

APPENDIX B: Tables and Figures

Table B-1: Summary of thermal properties of BTMS

S. N	Material Name	Density	Specific Heat	Thermal Conductivity	Electrical Conductivity	Data Sources
1.	Cell	2841.51	1040	24.8/1.17	-	Datasheet, (Koller et al., 2022)
2.	Aluminum	2719	871	202.4	3.541e+07	Ansys Database
3.	Air	1.225	1006.43	0.0242	-	Ansys Database
4.	Nickel	8900	460.6	91.74	1.282E+7	Ansys Database
5.	Wood	700	2310	0.173	1	Ansys Database
6.	Polyamide Tape	1420	1090	0.12	10e-15	(KAPTON, n.d.)

Table B-2: Liquid coolant details(Roe et al., 2022)

S. N	Material	Density (kg/m3)	Specific Heat(J/kgK)	Thermal Conductivity(W/mK)	Viscosity (kg/m-s)
1.	Water-Glycol (1:1) mix	1080	3473	0.4	0.005292

Table B-3: Temperature data at different velocity

Time	Natural cooling	Cooling at 1.3 m/s	Cooling at 3.2 m/s	Cooling at 4.3 m/s
1	26.3	24.6	23.35	22.45
2	26.95	24.75	23.1	22.1
3	27.75	24.65	22.95	22.05
4	28.05	24.85	22.85	22.25
5	28.6	24.8	22.85	21.95
6	29	24.8	22.8	22
7	29.3	24.65	22.8	21.95
8	29.8	24.6	22.85	21.95
9	29.9	24.55	22.7	21.95
10	30.15	24.5	22.6	21.95
11	30.2	24.45	22.55	22
12	30.4	24.3	22.55	21.9
13	30.6	24.3	22.35	21.65
14	30.95	24.15	22.4	21.8
15	30.85	24.1	22.35	21.4
16	30.9	24.1	22.2	21.65
17	30.85	23.9	22.1	21.4
18	30.8	24	22.1	21.6
19	30.75	23.75	22.1	21.5
20	30.7	23.8	22	21.3

Table B-4:Cell specification

Brand:	SAMSUNG
Model:	(INR18650-25S)
Cell Dimension:	Cell height: 65mm Cell diameter: 18.63mm
Capacity:	2500mAh Rated
Voltage:	3.60V Nominal
Weight:	47g max
Charging:	4.20V Maximum 1250mA Standard
Discharging:	2.50V Cutoff
Date of Production:	Mon Jul 01, 2019

APPENDIX C: Experimental Setup

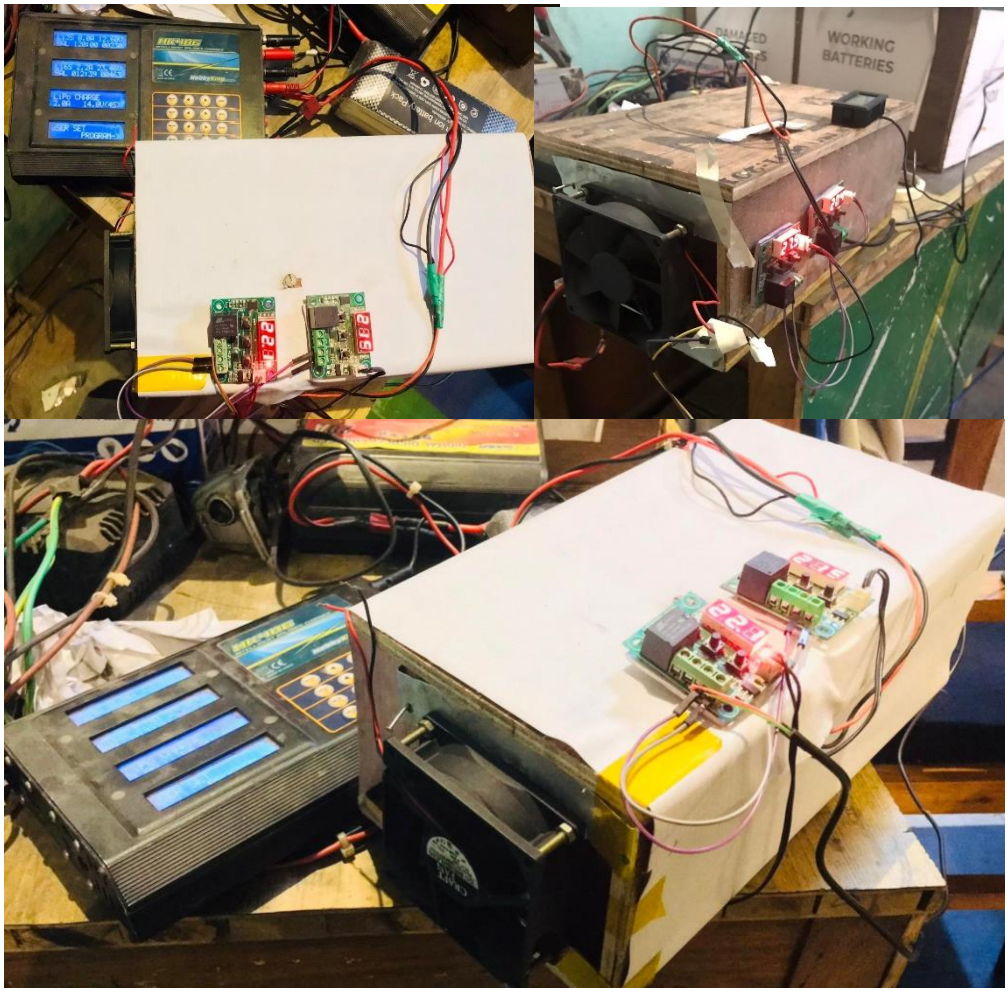

Figure C-1: Battery experiment setup images

STUDY AND DESIGN OF THERMAL MANAGEMENT SYSTEM OF LITHIUM-ION BATTERY MODULE

ORIGINALITY REPORT

3%
SIMILARITY INDEX

PRIMARY SOURCES

1	Pranjali R. Tete, Mahendra M. Gupta, Sandeep S. Joshi. "Developments in battery thermal management systems for electric vehicles: A technical review", Journal of Energy Storage, 2021 Crossref	68 words — 1%
2	www.mdpi.com Internet	58 words — < 1%
3	Weixiong Wu, Shuangfeng Wang, Wei Wu, Kai Chen, Sihui Hong, Yongxin Lai. "A critical review of battery thermal performance and liquid based battery thermal management", Energy Conversion and Management, 2019 Crossref	54 words — < 1%
4	Jinhong Xie, Zijing Ge, Mengyan Zang, Shuangfeng Wang. "Structural optimization of lithium-ion battery pack with forced air cooling system", Applied Thermal Engineering, 2017 Crossref	39 words — < 1%
5	www.databridgemarketresearch.com Internet	20 words — < 1%
6	Shuaihua Liu, Xunliang Liu, Ruifeng Dou, Wenning Zhou, Zhi Wen, Lin Liu. "Experimental and simulation study on thermal characteristics of 18,650 lithium–	17 words — < 1%